Published in final edited form as:
Neuroscience. 2013 November 12; 0: 468–488. doi:10.1016/j.neuroscience.2013.07.056.

Morphologically mixed chemical-electrical synapses formed by primary afferents in rodent vestibular nuclei as revealed by immunofluorescence detection of connexin36 and vesicular glutamate transporter-1

James I. Nagy[a], **Wendy Bautista**[a], **Brian Blakley**[b], and **John E. Rash**[c]

[a]Department of Physiology, Faculty of Medicine, University of Manitoba, Winnipeg, Canada

[b]Department of Otolaryngology, Health Sciences Centre and University of Manitoba, Winnipeg, Canada

[c]Department of Biomedical Sciences, Colorado State University, Fort Collins, Colorado, USA

Abstract

Axon terminals forming mixed chemical/electrical synapses in the lateral vestibular nucleus of rat were described over forty years ago. Because gap junctions formed by connexins are the morphological correlate of electrical synapses, and with demonstrations of widespread expression of the gap junction protein connexin36 (Cx36) in neurons, we investigated the distribution and cellular localization of electrical synapses in the adult and developing rodent vestibular nuclear complex, using immunofluorescence detection of Cx36 as a marker for these synapses. In addition, we examined Cx36 localization in relation to that of the nerve terminal marker vesicular glutamate transporter-1 (vglut-1). An abundance of immunolabelling for Cx36 in the form of Cx36-puncta was found in each of the four major vestibular nuclei of adult rat and mouse. Immunolabelling was associated with somata and initial dendrites of medium and large neurons, and was absent in vestibular nuclei of Cx36 knockout mice. Cx36-puncta were seen either dispersed or aggregated into clusters on the surface of neurons, and were never found to occur intracellularly. Nearly all Cx36-puncta were localized to large nerve terminals immunolabelled for vglut-1. These terminals and their associated Cx36-puncta were substantially depleted after labyrinthectomy. Developmentally, labelling for Cx36 was already present in the vestibular nuclei at postnatal day 5, where it was only partially co-localized with vglut-1, and did not become fully associated with vglut-1-positive terminals until postnatal day 20 to 25. The results show that vglut-1-positive primary afferent nerve terminals form mixed synapses throughout the vestibular nuclear complex, that the gap junction component of these synapses contain Cx36, that multiple Cx36-containing gap junctions are associated with individual vglut-1 terminals and that the development of these mixed synapses is protracted over several postnatal weeks.

Keywords

Electrical synapses; neuronal gap junctions; vesicular glutamate transporter-1

Address for correspondence, Dr. James I. Nagy, Department of Physiology, Faculty of Medicine, University of Manitoba, 745 Bannatyne Ave, Winnipeg, Manitoba, Canada R3E 0J9, nagyji@ms.umanitoba.ca, Tel. (204) 789-3767, Fax (204) 789-3934.

The long debate during the first half of the last century centering on whether inter-neuronal communication in the central nervous system (CNS) occurred by chemical or electrical means culminated around mid century with the demonstration of chemical transmission, followed shortly thereafter by the discovery of electrical transmission (reviewed in Bennett, 1977; Cowan Kandel, 2001). The morphological substrate of (most) electrical synapses was identified to be neuronal gap junctions that form at close plasma membrane appositions and consist of connexin channel-forming proteins that allow intercellular movement of ions and small molecules (Bennett, 1997). While initially considered a less sophisticated form of communication widely utilized only in submammalian species (see however, Bennett, 2000), evidence slowly accumulated indicating electrical transmission between mammalian neurons in numerous CNS regions (see Nagy and Dermietzel, 2000). Nevertheless, it has been only in the past decade, with renewed interest in the area, that the importance and functional relevance of electrical transmission in mammalian CNS has become generally accepted (Bennett and, Zukin, 2004; Connors and Long, 2004; Hormuzdi et al., 2004; Sohl et al., 2005; Meier and Dermietzel, 2006). Nearly all neuronal gap junctions so far identified in mammalian CNS occur at appositions between dendrites, somata or dendrites and somata. However, electrical communication can also occur between nerve terminals and postsynaptic elements; in fact, nerve terminals were among the first structures at which electrical transmission was found (Furshpan, 1964; reviewed in Bennett and Goodenough, 1978). Synaptic terminals with capabilities for electrical and chemical transmission, termed mixed synapses, have been extensively studied in lower vertebrates, among which the best characterized are the club endings on giant Mauthner cells in goldfish (Pereda et al., 2003,2004). Morphological and/or electrophysiological evidence for morphologically mixed synapses has been reported in only a few locations in mammalian CNS, including rat lateral vestibular nucleus (LVN) (Sotelo and Palay, 1970; Korn et al., 1973; Wylie, 1973; Sotelo, 1975; Sotelo and Korn, 1978; Sotelo and Triller, 1981), spinal cord (Rash et al., 1996) and hippocampus (Vivar et al., 2012; Hamzei-Sichani et al., 2012; Nagy, 2012).

In the LVN of rat, as well as mouse (cited as unpublished observations in Sotelo and Korn, 1978), gap junctions are formed between large nerve terminals and either the somata or dendrites of large neurons that themselves appear not to be directly coupled by interdendritic or soma-somatic gap junctions (Sotelo and Palay, 1970; Korn et al., 1973). Similar observations have been made in the vestibular nuclei or their anatomical equivalent in lower vertebrates, including lamprey (Stefanelli and Caravita, 1970), goldfish (Hinojosa, 1973), toadfish (Korn et al., 1977), frog (Sotelo, 1977) and chick (Hinojosa and Robertson, 1967; Peusner, 1984). The terminals forming gap junctions in these species as well as in rat are either known or have been inferred to be of primary afferent origin based on demonstrations of electrical transmission by vestibular primary afferents in toadfish (Korn et al., 1977), frog (Precht et al., 1974; Babalian and Shapovalov, 1984), lizard (Richter et al., 1975), pigeon (Wilson and Wylie, 1970) and rat (Wylie, 1973). Nearly four decades after these early studies, mixed synapses in vestibular nuclei have received little attention, although glutamatergic transmission by primary afferents in these nuclei have been well studied (Highstein and Holstein, 2006). In the mammalian vestibular nuclear complex, there is no anatomical information available on the distribution and density of neuronal gap junctions, the connexin constituents of these junctions, or the source of terminals forming mixed synapses.

The family of connexin proteins that form gap junctional intercellular channels consists of twenty or twenty-one family members. The discovery that connexin36 (Cx36) is expressed in neurons (Condorelli et al., 1998; Söhl et al., 1998) has enabled histochemical approaches to demonstrate widespread neuronal expression of Cx36 in mammalian CNS, including Cx36 mRNA expression in neurons of rodent vestibular nuclei (Condorelli et al., 2000). In

our studies of Cx36 protein expression in brain and spinal cord, the anti-Cx36 antibodies used provide robust immunofluorescence labelling of Cx36 associated with neurons, and we have established the specificity of these antibodies in various CNS regions using Cx36 knockout (ko) mice (Li et al., 2008; Curti et al., 2012; Bautista et al., 2012). Immunolabelling of Cx36 occurs exclusively as immunopositive puncta, with no detection of intracellular labelling. We have confirmed that this punctate labelling corresponds to sites where we detect ultrastructurally-identified neuronal gap junctions (Rash et al., 2000; 2001; Nagy et al., 2004; Rash et al., 2007a,b; Li et al., 2008). Further, there is a high correlation between presence of Cx36 and presence of functional electrical synapses (Bennett and, Zukin, 2004; Connors and Long, 2004; Hormuzdi et al., 2004). While we cannot discount the possibility that additional connexins may be expressed in neurons, our studies have excluded neuronal localization of a variety of connexins expressed in the CNS (Rash et al., 2000, 2001, 2007a, b; Curti et al., 2012). Taken together, these points allow use of immunofluorescence labelling of Cx36 as the current best marker for electrical synapses in most regions of the mammalian CNS. Here, we describe abundant immunolabelling of Cx36 in vestibular nuclei of adult and developing rat and mouse, and report on the association of Cx36 with the nerve terminal marker vesicular glutamate transporter-1 (vglut-1). In addition, studies were undertaken to determine whether Cx36 association with vglut-1 in the vestibular nuclear complex reflects localization of Cx36 terminals of primary afferent origin.

EXPERIMENTAL PROCEDURES

Animals and antibodies

Animals used in this study included a total of forty-four adult Sprague-Dawley rats. For developmental studies, three rats were used at postnatal day 5, two at postnatal day 10, three at postnatal day 15, two at postnatal day 20, three at postnatal day 25 and the rest as adults. Included were fourteen adult rats taken for surgical procedures involving labyrinthectomy and vestibular nerve section. Mouse strains used included fourteen adult CD1 mice, three of these mice at postnatal day 5, and three at postnatal day 10 and the rest as adults. In addition, colonies of C57 BL/6-129SvEv wild-type and Cx36 ko mice were established at the University of Manitoba through generous provision of wild-type and Cx36 ko breeding pairs from Dr. David Paul (Harvard). Five adult wild-type and three adult ko mice were used from these colonies. Expression of Cx36 protein was investigated in the vestibular nuclei of both rat and mouse, because some early studies relevant to neuronal gap junctions in these nuclei were conducted in rat, and because examination of mouse provides the opportunity to confirm antibody specificity of Cx36 detection using wild-type *vs.* Cx36 ko mice. Studies were also conducted on brains harvested from three adult cats and three adult Hartley guinea pigs. Tissues from some of the animals were employed in parallel unrelated studies; therefore the numbers indicated do not reflect total cumulative usage in separate publications from our laboratory. Animals were utilized according to approved protocols by the Central Animal Care Committee of University of Manitoba, with minimization of the numbers of animals used.

Two polyclonal antibodies (Cat. No. 36–4600 and Cat. No. 51–6300) and one monoclonal antibody (Cat. No. 39–4200) against Cx36 were obtained from Life Technologies Corporation (Grand Island, NY, USA) (formerly Invitrogen/Zymed Laboratories), and have been previously characterized for specificity of Cx36 detection in various regions of rodent brain (Li et al., 2004; Rash et al., 2007a,b; Curti et al., 2012). These were used at a concentration of 1–2 μg/ml in primary antibody incubations with tissue sections. Other antibodies included a guinea pig polyclonal anti-vglut-1 obtained from Millipore (Temecula, CA, USA) and used at a dilution of 1:1000, and a mouse monoclonal anti-bassoon antibody obtained from Stressgen Bioreagents (Victoria, BC, Canada) and used at a dilution of 1:1000. Secondary antibodies included Cy3-conjugated goat or donkey anti-mouse IgG

diluted 1:600 (Jackson ImmunoResearch Laboratories, West Grove, PA, USA), Alexa Flour 488-conjugated goat or donkey anti-rabbit and anti-mouse IgG diluted 1:600 (Molecular Probes, Eugene, OR, USA), and Cy5-conjugated goat anti-mouse IgG diluted 1:500 (Jackson ImmunoResearch Laboratories). All antibodies were diluted in 50 mM Tris-HCl, pH 7.4, containing 1.5% sodium chloride (TBS) and 0.3% Triton X-100 (TBSTr) containing 10% normal goat or normal donkey serum.

Tissue preparation

Animals were deeply anesthetized with equithesin (3 ml/kg) and placed on a bed of ice. Most rats and mice 15 days of age and older were perfused transcardially with 0.1–0.2 ml per gram body weight of cold (4°C) pre-fixative consisting of 50 mM sodium phosphate buffer, pH 7.4, 0.1% sodium nitrite, 0.9% NaCl and 1 unit/ml of heparin. This was followed by perfusion with 0.5 to 1 ml per gram body weight of fixative solution containing cold 0.16 M sodium phosphate buffer, pH 7.4, 0.2% picric acid and either 1% or 2% formaldehyde from freshly depolymerized paraformaldehyde. Animals were then perfused with 0.1–0.2 ml per gram body weight of a cold solution containing 10% sucrose and 25 mM sodium phosphate buffer, pH 7.4, to wash out excess fixative. Cats and guinea pigs were similarly anesthetized followed by transcardiac perfusion. Brains were removed and stored at 4°C for 24–48 h in cryoprotectant containing 25 mM sodium phosphate buffer, pH 7.4, 10% sucrose, 0.04% sodium azide.

It should be noted that optimal immunohistochemical detection of Cx36 required the weak tissue fixations conditions described above. This posed a problem for double immunofluorescence labelling of Cx36 in combination with vglut-1, because optimal labelling of vglut-1 required stronger fixation (> 2% formaldehyde), leaving only a narrow window of fixation strength where maximal levels of both proteins could be reliably detected. To achieve this window, volumes of fixative (1 or 2% formaldehyde) for perfusion were varied in the range noted above. To ensure that Cx36 and vglut-1 detection in double-labelled sections was adequate at the perfusion volumes chosen, quality of labelling for Cx36 and vglut-1 in those sections was compared with optimal labelling for Cx36 in more weakly fixed sections, and with optimal labelling for vglut-1 in more strongly fixed sections. Given these considerations, some variability in immunolabelling quality might be expected and was encountered.

Most brains from mice less than 15 days of age were prepared by immersion fixation; animals were deeply anesthetized as above, decapitated, and the brains were removed and placed for 20 to 30 min into fixative containing 0.16 M sodium phosphate buffer, pH 7.4, 2% freshly depolymerized paraformaldehyde and 0.2% picric acid. The quality of immunohistochemical detection of proteins of interest after immersion fixation was equal to that observed after transcardial perfusion, as deduced from examination of brains from some postnatal day 10 animals prepared by cardiac perfusion and some brains from adult animals prepared by immersion fixation. After fixation, brains were transferred to cryoprotectant for a minimum of 1 to 2 days as above. Due to the weak tissue fixation conditions used, brains were taken for sectioning no longer than a few days after cryoprotection; longer storage of unsectioned brains led to deterioration of tissues, poor quality of sections and suboptimal immunohistochemical results. Transverse sections of brainstem were cut at a thickness of 10–15 μm using a cryostat and collected on gelatinized glass slides. Slide-mounted sections could be routinely stored at −35 °C for several months before use.

Light microscope immunofluorescence

Slide mounted sections were removed from storage, air dried under a fan for 10 min, and then washed for 20 min in TBSTr. Sections were processed for immunofluorescence

staining, as previously described (Li et al., 2008; Bautista et al., 2012; Curti et al., 2012). For single immunolabelling, sections were incubated for 24 h at 4°C with anti-Cx36, then washed for 1 h in TBSTr and incubated with appropriate secondary antibody for 1.5 h at room temperature. The same incubation procedures were used for double and triple immunofluorescence labelling, except that sections were incubated simultaneously with two or three different primary antibodies generated in different species, washed, and incubated simultaneously with two or three appropriate secondary antibodies. Some sections processed for single or double immunolabelling were counterstained with either green Nissl fluorescent NeuroTrace (stain N21480) or Blue Nissl NeuroTrace (stain N21479) (Molecular Probes, Eugene, OR, USA). All sections were coverslipped with the antifade medium Fluoromount-G (SouthernBiotech, Birmingham, AB, USA). Control procedures, involving omission of one of the primary antibodies with inclusion of the secondary antibodies used for double and triple labelling, indicated absence of inappropriate cross-reactions between primary and secondary antibodies for all of the combinations used in this study.

Immunofluorescence was examined on a Zeiss Axioskop2 fluorescence microscope, using Axiovision 3.0 software (Carl Zeiss Canada, Toronto, Ontario, Canada) for capturing images, and a Zeiss 710 laser scanning confocal microscope using ZEN 2010 image capture and analysis software. Data from wide-field and confocal microscopes were collected either as single scan images or z-stack images with multiple scans capturing a thickness of 2 to 14 μm of tissue at z scanning intervals of typically 0.4 to 0.6 μm. Images of immunolabelling obtained with Cy5 fluorochrome were pseudo colored blue. Final images were assembled according to appropriate size and adjusted for optimal signal to noise presentation using CorelDraw Graphics (Corel Corp., Ottawa, Canada) and Adobe Photoshop CS software (Adobe Systems, San Jose, CA, USA). Movie files were constructed using Zeiss ZEN software.

Quantitative analyses

Sections double-labelled for Cx36 and vglut-1 were taken for measurements of diameters of Cx36-puncta, diameters of vglut-1-positive terminals with which these puncta were associated, and the diameters of clusters of Cx36-puncta associated with these terminals. Subsets of fifty Cx36-puncta, fifty vglut-1-positive terminals and twenty clusters of Cx36-puncta distributed on somata and dendrites of neurons in the vestibular nuclei from three rats were taken for measurements using Zen quantitative software tools (Zeiss Canada). The diameters of vglut-1-positive terminals (n = 20) localized on the surface of neuronal somata in the LVN of cat were also measured. Similar double-labelled sections were taken for quantitative analysis of the numbers of Cx36-immunopositive puncta associated with individual vglut-1-positive nerve terminals on neurons in the vestibular nuclei. In each of four adults rats, confocal immunofluorescence images ranging from 17 to 19 fields of LVN were collected at sufficient magnification, using a x60 objective lens, to resolve and visualize individual Cx36-puncta. This required collection of z-stack images to ensure capture of all puncta associated with terminals in the z-axis. The number of Cx36-puncta contained within large vglut-1-positive terminals seen *en face* overlying neuronal somata and dendrites were counted in images from each of the four animals; terminals viewed on edge at the periphery of somata and dendrites were omitted from analysis. The data for each animal was then normalized by calculating the percentage of terminals displaying particular numbers of puncta, and the number of terminals containing particular numbers of puncta was then averaged over the four animals and expressed as mean ± s.e.m.

Sections double-labelled for vglut-1 and Cx36 were used from four rats to capture images for determining numbers of Cx36-puncta associated with individual vglut-1-positive terminals in the LVN. The number of puncta localized to each of a total of 1,782 terminals

was counted. The percentages of terminals displaying particular numbers of puncta were separately plotted for each rat, and the average percentage of terminals displaying a given number of puncta was calculated (mean ± s.e.m.) from the four rats.

Vestibular labyrinthectomy and nerve lesions

Rats taken for unilateral labyrinthectomy and vestibular nerve section were anesthetized with a mixture of isofluorane and oxygen for induction and maintenance of anaesthesia, with delivery of gas through a nose cone. Respiratory and pulse rate were monitored with an infrared oximeter clipped to one forepaw. Temperature was maintained at 37°C with a heating blanket and monitored via a rectal thermometer. Rats were placed on a lateral supine position, and the mandibular area below the left ear was shaved and sanitized with betadine prior to placing sterile drapes. Using a lateral approach, incisions were made perpendicular into the external auditory canal, and fibromuscular and cartilage tissues were dissected with blunt scissors to expose the tympanic bulla lying lateral and superior to the digastric muscle. Once the tympanic bulla was visualized with the aid of a surgical microscope, a drill (head size 0.5 mm) was used to expose the tympanic membrane and the stapes, and to open the tympanic bulla to expose the cochlea, with caution to avoid damage to the stapedial artery lying at the base of the cochlea. When present, bleeding from this artery was controlled by using the hemostatic agent Avitene, gauze pressure or cauterization. This was followed by performing vestibular nerve section via transcochlear ablation and/or Scarpa ganglionectomy. Some animals received cochlea and vestibular nerve ablation, with or without an attempt at complete ganglionectomy. Nerve and ganglion ablation was approached by cauterization in the area of the internal auditory meatus using a high temperature, fine tip, extended shaft micro-ophthalmic cauterization device (Bovie Medical Corp., Clearwater, Florida, USA), or by penetrating this area using a small hooked needle to ablate Scarpa's ganglion at its attachment to the proximal end of the vestibular nerve. The surgical site was packed with Avitene, sutured, and animals were maintained for a survival time of 7–9 days. During recovery, rats displayed various degree of deficits in balance, head tilting, and weight support, lasting for a few days or throughout the survival period, but all recovered to be able to stand and walk. Pain was controlled with buprenorphine (intramuscular, 0.03–0.06 ml/kg) every 8 hours for two days post-surgery.

Tissues from animals subject to unilateral labyrinthectomy were prepared for immunohistochemistry as described above. In comparisons of labelling for vglut-1 and Cx36 in sections of vesticular nuclei on the unoperated *vs.* lesion side, the intact side of each animal served as the basis for comparison of the effect of deafferentation on the contralateral lesion side. This effectively reduced confounding results that may have been introduced by variablilty of tissue fixation quality among animals. Further, during image acquisition of labelling, the control side was first photographed at an optimal exposure time setting, and the lesioned side was then photographed at the same exposure time to allow unbiased comparison of immunolabelling intensity on the control *vs.* lesioned side.

RESULTS

Distribution and cellular localization of Cx36 in vestibular nuclei

The distribution and cellular localization of Cx36 was examined by immunofluorescence labelling in each of the nuclei comprising the vestibular nuclear complex in adult rat and mouse. This complex consists of the spinal (SpVN), lateral (LVN), medial (MVN) and superior (SuVN) vestibular nuclei, with the MVN further subdivided into the more laterally located MVN magnocellular part (MVNmc) and the medially located MVN parvicellular part (MVNpc). An overall view of immunolabelling for Cx36 in adult rat LVN is presented at low magnification in Figure 1, with Cx36 immunofluorescence alone shown with red

label in the left column of images to provide unobscured visualization of labelling, and the same fields shown as overlay with fluorescence Nissl counterstaining (green) in the right column to provide a background cellular context to the labelling. In comparison with most, though not all *[(e.g.*, sexually dimorphic motor nuclei in spinal cord (Bautista et al., 2013)], other adult rodent brain regions in which we have examined immunolabelling of Cx36, such as cerebral cortex, striatum, midbrain and cerebellum (not shown), labelling intensity and density was remarkably greater in the vestibular nuclear complex. Immunolabelling was detected in each of the vestibular nuclei, as shown in the SpVN (Fig. 1A), the LVN (Fig. 1B), the MVNmc (Fig. 1C) and the SuVN (Fig. 1D), but was very sparse in the MVNpc, which is populated by relatively small neurons (Fig. 1C). With one exception, immunolabelling was localized to neurons and typically reflected the distribution of large- and medium-size neuronal somata in the four major nuclear divisions, so much so that locations of these neurons could invariably be inferred from visualization of Cx36 immunofluorescence alone *(i.e.*, in the absence of Nissl staining). This is especially remarkable given that Cx36 detectable by immunofluorescence in these vestibular nuclei is likely localized exclusively to gap junctions, as discussed below. The one exception was observed in the dorsocaudal portion of the LVN, which is populated by somewhat larger and more numerous neurons than seen in the rostroventral LVN, but was found to be largely devoid of immunolabelling for Cx36, except for a few sparse puncta per section (Fig. 1B). These dorsally located neurons have typically been included as part of the LVN, notwithstanding considerations regarding their somewhat distinct anatomical and functional relationships (Brodal, 1981). The uniform absence of Cx36 association with these neurons further distinguishes them from all other large neurons in the vestibular nuclei, and suggests that they may represent at least a functionally distinct set of neurons.

A higher magnification view of Cx36 immunofluorescence in each of the vestibular nuclear divisions of adult rat brain, shown with Nissl fluorescence overlay, is presented in Figure 2. Here, several features of labelling for Cx36 are evident. First, labelling in the LVN (Fig. 2A), SpVN (Fig. 2B) and MVNmc (Fig. 2C) is often associated with the somata and initial dendrites of medium and large size neurons. Second, it is clear that the parvicellular part of the MVN nucleus is largely devoid of labelling (Fig. 2D, MVNpc indicated by asterisk), compared with association of labelling around large neurons in the laterally located MVNmc (Fig. 2D, arrows). Third, there is a heterogeneity of labelling among large neurons in the LVN (Fig. 2E) and MVNmc (Fig. 2F) as well as SpVN (not shown), such that neurons bearing little or no labelling for Cx36 are intermingled with similarly large neurons displaying an abundance of Cx36 immunofluorescence around their periphery. And fourth, in contrast to patterns of Cx36 association with large neurons in other vestibular nuclei, the typically smaller neurons characteristic of the SuVN displayed labelling of Cx36 mostly on their initial dendrites rather that cell bodies (Fig. 2G). Details of these patterns of labelling are described more fully below.

In general, results on Cx36 distribution and cellular localization in vestibular nuclei of mouse were similar to those described above in rat. Examples of Cx36 immunofluorescence in mouse are shown with red label alone, and with green Nissl fluorescence overlay in the SpVN (Fig. 3A), MVNmc (Fig. 3B) and LVN (Fig. 3C). In each region, labelling of Cx36 is seen surrounding neuronal somata and extending along initial dendrites. As in rat, labelling was more often associated with large *vs.* small neuronal cell bodies. A low magnification view midway through a large part of the LVN from a wild-type mouse is shown in Figure 3D, where it is evident that intense labelling for Cx36 is distributed throughout the nucleus. A corresponding field of the LVN photographed in a brain section from a Cx36 knockout mouse after processing with the same anti-Cx36 antibody as used in Figure 3D, shows a total absence of immunofluorescence signal (Fig. 3E), indicating specificity of Cx36 detection. A similar absence of labelling was seen in the other vestibular nuclei of Cx36 ko

mice. Similar results were obtained with each of the anti-Cx36 antibodies used in this study. We have emphasized elsewhere (Li et al., 2008; Curti et al., 2012) that detection of Cx36 with these antibodies is especially sensitive to tissue fixation conditions, and that optimal detection requires the weak fixations used here. Use of stronger fixations, including 4% formaldehyde, with or without post-fixation, obliterated Cx36 immunofluorescence signal.

In contrast to the profuse immunolabelling of Cx36 in vestibular nuclei of rodent brain, we failed to detect any labelling of this connexin in these nuclei of either guinea pig or cat brain (not shown). These negative results were not due to failure of anti-Cx36 antibody to recognize a possibly different amino acid sequence corresponding to the antibody epitope of Cx36 in these species, because robust labelling of Cx36 was observed in the inferior olivary nucleus of both guinea pig and cat, images of which were presented as positive controls for Cx36 detection in the original submission of this report, together with comparisons of labelling for Cx36 in the inferior olive of rat and mouse, which are known to harbor an abundance of Cx36-containing neuronal gap junctions (Hoge et al., 2010). Dense labelling for Cx36 was also seen in the molecular layer of the cerebellum in guinea pig and cat (not shown), which typically contains an abundance of Cx36-puncta in rodents (not shown).

Confocal analysis of Cx36 immunofluorescence

Examination of Cx36 immunofluorescence by laser scanning confocal microscopy (Fig. 4; Cx36 red, with or without green Nissl fluorescence overlay) revealed several features of labelling alluded to above. First and foremost is that labelling for Cx36 appeared exclusively as immunopositive puncta (Cx36-puncta), similar to the appearance of antibody detection of Cx36 protein that we have described in other regions of rodent brain (Li et al., 2004, 2008; Rash et al., 2007a,b; Bautista et al., 2012; Curti et al., 2012). Second, no labelling of either a punctate or diffuse nature was detected intracellularly; labelling was always localized to cell surfaces, presumably plasma membranes. This point is less evident in the z-stack images presented in Figure 4A–J, which instead aimed to capture the totality of Cx36-puncta associated with neuronal elements. However, single confocal scans through the center of neuronal somata showed the occurrence of labelling only around their periphery, and scans through their top or bottom edge indicated labelling only at the cell body surface (Fig. 4K,L). And third, comparison of intracellular fluorescence signal in vestibular neurons from wild-type *vs.* Cx36 ko mice revealed little difference in intensity (not shown), presumably due either to normally very low levels of Cx36 in neuronal cytoplasmic compartments, or to inability of the anti-Cx36 antibodies we use to detect Cx36 in the course of its intracellular trafficking to and from the plasma membrane, at least under the tissue fixation conditions used here. It should be noted that our choise of fixation for the present work does not account for the lack of cytoplasmic staining for Cx36, because we do not detect cytoplasmic Cx36 immunoreactivity (i.e., greater than seen in Cx36 ko mice) under any fixation conditions among dozens tested.

Examples of Cx36-puncta associated with individual neurons are shown in Figure 4A–C. Some neurons displayed puncta distributed over the entirety of their surface and relatively large initial dendrites (Fig. 4A; shown with Nissl counterstaining in inset). Equally often, neurons and dendrites were seen bearing roughly round or oval patches of Cx36 immunofluorescence, which were much larger than individual puncta (Fig. 4B). Through focus analysis indicated that, like all Cx36 immunosignal, these patches were localized to neuronal surfaces. At higher magnification (Fig. 4C; shown with Nissl counterstaining in inset), the patches were seen to consist of numerous puncta assembled into clusters, with channel free areas surrounding puncta in these clusters. Puncta contained in clusters appeared to be randomly organized and varied considerably in size, as shown in Figure 4D, but otherwise had an appearance similar to those dispersed individually over neuronal

surfaces (as in Fig. 4A). Clusters of Cx36-puncta had an average diameter of 4.2 ± 0.35 μm, and puncta whether in clusters or not had an average diameter of 0.65 ± 0.03 μm.

Frequently, what appeared to be linear arrangements of Cx36-puncta were observed around the perimeter of neuronal somata (Fig. 4C, double arrows), shown by a higher magnification z-stack image in Figure 4E. However, rotation of this image revealed that it, too, consisted of a cluster of Cx36-puncta. Thus, clusters of Cx36-puncta could be viewed on edge around the perimeter of cells when captured with their plane oriented perpendicular to the horizontal axis, or viewed *en face* when captured with their plane oriented parallel to the horizontal axis.

A feature examined in less detail, in the absence of corresponding ultrastructural analysis or more extensive dendritic counterstaining than provided by the Nissl approach used here, was the extent of Cx36 localization at appositions between neuronal elements, which could be indicative of sites of neuronal gap junctional coupling. Nevertheless, examples were found where dendritic elements heavily labelled for Cx36 appeared to pass very close to the somata of other neurons (Fig. 4G). In addition, very rare cases (three in hundreds of sections examined) were encountered where Cx36 was seen distributed at appositions between neuronal somata in the various vestibular nuclei (Fig. 4H–J). In each of these cases, the participating neurons were much smaller than the typically large neurons in these nuclei. These examples raise the possibility of Cx36 localization to dendro-somatic and soma-somatic elements, but equally possible is the association of these Cx36-puncta to nerve terminals sandwiched between these elements (discussed below).

Association of Cx36 with nerve terminals in vestibular nuclei

The dense immunofluorescence labelling of Cx36 associated with neuronal somata in the vestibular nuclei, together with the punctate appearance of labelling, suggests the possibility that Cx36 is localized to gap junctions in this structure, as supported by studies elsewhere in brain where correspondence of Cx36-puncta to ultrastructurally-identified neuronal gap junctions containing Cx36 has been reported (Li et al., 2004, 2008; Kamasawa et al., 2006; Rash et al. 2007a,b). This possibility is further supported by observations of neuronal gap junctions in the LVN, which were identified by thin-section electron microscopy (Sotelo and Palay, 1970; Korn et al. 1973). However, unlike other brain regions where neuronal gap junctions for the most part are found linking dendrites, those junctions in the LVN were found to occur at nerve terminals, linking pre- and postsynaptic elements and forming mixed chemical/electrical synapses (Sotelo and Palay, 1970; Korn et al. 1973). An example of this is presented here in Figure 5, reproduced from the early work of Korn et al. (1973) nearly forty years ago, showing an axon terminal that is packed with synaptic vesicles and that forms a gap junction with a postsynaptic dendrite (Fig. 5A), and a high magnification of a gap junction showing its heptalaminar appearance (Fig. 5B).

Based on the presence of mixed synapses in the LVN, we examined Cx36 immunofluorescence in relation to the localization of the nerve terminal marker vglut-1 in vestibular nuclei. Sections double-labelled for Cx36 (red fluorochrome) and vglut-1 (green fluorochrome), with Nissl fluorescence blue counterstaining, are shown in Figure 6. In adult rat LVN, neuronal cell bodies and initial dendritic segments that were heavily decorated with a high density of vglut-1-positive terminal boutons (Fig. 6A1) were equally laden with Cx36-puncta (Fig. 6A2). Overlay of images revealed substantial localization of Cx36-puncta at vglut-1-positive boutons (Fig. 6A3; with boxed area shown at higher magnification in Fig. 6B1–3). Similar results on Cx36-puncta co-localization with labelling for vglut-1 was obtained in adult mouse LVN (Fig. 6C1–3), as well as in adult rat and mouse SpVN, MVNmc and SuVN (not shown). While no attempt was made to quantify Cx36-puncta or vglut-1-positive terminal boutons associated with large *vs.* small neurons, or the extent of

total Cx36-puncta associated *vs.* unassociated with vglut-1-positive boutons, it was clear that the vast majority of Cx36-puncta were localized to large vglut-1-positive boutons contacting large neurons.

Laser scanning confocal examination of labelling for Cx36 (red signal) in combination with vglut-1 (green signal) is shown in Figure 7A–E. Two neuronal somata with thick initial dendritic segments outlined by immunofluorescence label are shown in Figure 7A (not counterstained, but centers of soma are marked by asterisks in image showing Cx36/vglut-1 overlay, and in inset image of the same field showing labelling for Cx36 alone). From this and similar images, measurements of vglut-1-positive terminals of all sizes on large neurons yielded an average diameter of 3.1 ± 0.16 μm. Nearly all of these terminals display yellow signal, representing red/green overlap. To confirm the extent of this overlap, and exclude the occurrence of Cx36-puncta lying above or below vglut-1-positive boutons in the z-stack image of Figure 7A, representing 14 μm in the z dimension, a movie with image rotation is provided as neuroimage 1, indicating that all Cx36-puncta remain associated with vglut-1-labelled terminals at various angles of rotation. Another neuronal somata covered with vglut-1-positive terminals is shown in an image at higher magnification in Figure 7B. Collections of Cx36-puncta are seen distributed within the confines of labelling for vglut-1. Thus, clusters of Cx36-puncta described in Figure 4 correspond to puncta associated with individual terminal boutons. However, the larger average diameter of the clusters (4.2 ± 0.35 μm) than the average diameter of all the typically round vglut-1-terminals seen on neurons suggests localization of clusters of Cx36-puncta to a subset of relatively larger vglut-1-containing terminals. On rare occasions, terminals specifically in LVN were seen having an extended configuration, with continuous labelling for vglut-1 and lengths of up to 15 μm (Fig. 7C), and these too displayed Cx36-puncta along their length.

Similar to the absence of detectable intracellular labelling of Cx36 in neuronal somata and dendrites noted earlier, Cx36 was not detected in the interior of terminals, but rather was associated with their peripheries, as determined by through focus analysis at high confocal magnification (not shown). This was also evident in 3D-rendered z-stack images (Fig. 7D), where vglut-1-positive terminals surrounding a dendritic initial segment (dendrite not counterstained, but centrally located and surrounded by terminals) display Cx36-puncta at their surface of contact with the dendrite, rather than throughout their surface or interior. This is better appreciated with image rotation, as provided in neuroimage 2.

The distribution of Cx36-puncta at individual terminals was examined in relation to both labelling intensity for vglut-1 and localization of the protein bassoon, a marker of presynaptic active zones for transmitter release (Richter et al., 1999). Immunolabelling for vglut-1 is often robust, but at sufficiently low confocal gain setting, terminals displayed a heterogeneous pattern of vglut-1 labelling intensity (Fig. 7E1). Cx36-puncta tended to be localized within terminal regions having faint vglut-1 labelling, suggesting that vglut-1-containing vesicles tend to accumulate least in plasma membrane regions that harbor Cx36-containing gap junctions, where vesicles release would be obstrcuted by the gap junctions. Similarly, while Cx36-puncta were intermingled with punctate labelling for the active zone marker bassoon within vglut-1-positive terminals, there was no overlap between labelling for Cx36 and bassoon (Fig. 7F and G), again indicating separate localization of the functionally different structures represented by these proteins.

There was a wide variation in the numbers of Cx36-puncta associated with large vglut-1-positive boutons. Counts of the number of these puncta localized to individual large terminals was determined from examination of a total of 932 terminals containing a total of 5,836 puncta in the vestibular nuclei of four rats. The results, expressed as percentage of terminals containing particular numbers of puncta averaged over data collected from the

four rats, are plotted in the histogram shown in Figure 8. A relatively small proportion (7%) of large vglut-1-positive boutons were devoid of Cx36-puncta, but false negative results could not be ruled out in these cases *(e.g.*, failure to detect faint Cx36-puncta or puncta out of the plane of visualization in relation to the terminal). It was further calculated that 7% of vglut-1-positive terminals displayed only a single Cx36-punctum, 53% displayed 2 – 7 puncta, 26% displayed 8 −15 puncta, and the remaining 7% displayed greater than 16 of these puncta.

Development of Cx36 expression in vestibular nuclei

To determine whether Cx36 associated with mixed synapses in vestibular nuclei exhibits similar or different developmental patterns of expression compared with Cx36 at pure electrical synapses (*e.g.*, dendro-dendritic) occurring elsewhere in brain, we examined immunolabelling of Cx36 and vglut-1 in these nuclei of rat and mouse at various postnatal ages. Results from rat are shown in Figures 9 and 10, where the labelling scheme with fluorochromes is the same as that in Figure 6. At postnatal day 5 in the LVN, labelling for both proteins was already present and these labels were co-localized to a limited extent, mostly on neuronal somata (Fig. 9A). Many neurons, however, were devoid of labelling (Fig. 9A3), and some neurons bearing label for both Cx36 and vglut-1 displayed minimal co-localization of the proteins (Fig. 9B). In addition, individual Cx36-puncta not associated with neuronal somata were seen sparsely distributed throughout the nucleus (Fig. 9A3). The pattern of labelling in the LVN at postnatal day 10 (not shown) was similar to that seen at postnatal day 15 (Fig. 9C); the density of Cx36 and vglut-1 label on neurons was increased, but the labels were not yet fully co-localized to the extent seen in the LVN of adults, as shown by higher magnification of labelling at postnatal day 15 in Figure 9D, and by overlay of labelling for vglut-1 and Cx36 without counterstaining in Figure 9E. In view of these findings, animals at postnatal day 20 and 25 were examined, results from which revealed that the adult pattern of labelling was reached largely by the earlier and fully by the latter of these ages. Similar developmental profiles of Cx36 and vglut-1 labelling were observed in the SuVN and the MVNmc of rat, and in the vestibular nuclei of mouse at postnatal days 5 and 10 (not shown).

Labelling in the SpVN rat paralleled that in the LVN qualitatively; at early ages, widely dispersed individual Cx36-puncta unassociated with vglut-1 were present at postnatal day 5, persisted till postnatal day 15 (Fig. 10), and then were largely absent by postnatal day 20. Co-localization of Cx36 with vglut-1 was evident at the earliest age, continued to increase, and reached an adult appearance by postnatal day 20. However, the density of labelling for both Cx36 and vglut-1 at postnatal day 5 and 10 (not shown) was greater than observed in the LVN at these ages, and the extent of Cx36/vgut-1 co-localization was much greater at each of the ages examined during the first two postnatal weeks, as shown in Fig. 10. The more rapid approach to the adult appearance of labelling in the SpVN *vs.* LVN was not an artifact of differential tissue fixation, because data from the two adjacent nuclei in brain were derived from the same tissues. The slightly earlier adult appearance of Cx36 and vgut-1 in the SpVN suggests earlier maturation of functions associated with this nucleus, which is consistent with the rostro-caudal gradient in the maturation of posture and locomotion in rat (Clarac et al., 1998), and the greater projections of the SpVN to rostral vs. caudal spinal cord levels (Goldberg et al., 2012).

Vglut-1 and Cx36 in vestibular nuclei after labyrinthectomy

The effect of labyrinthectomy, involving unilateral ablation of the Scarpa's sensory ganglion and/or its associated vestibular nerve root, on immunolabelling of vglut-1 and Cx36 in the vestibular nuclei is shown in Figure. 11. Of the fourteen rats taken for labyrinthectomy, six were used to develop and refine the surgical approach, and these gave variable results, with

either no effect on vglut-1 and Cx36 labelling in the vestibular nuclei or loss of labelling ranging from an estimated 20–50% (based on visual inspection) in some but not all of these nuclei. Among the other nine animals, loss of labelling was somewhat greater in two rats, but still not complete. The best results were obtained in animals where a complete Scarpa ganglionectomy was attempted followed by ablation of its vestibular nerve root. The data presented here are representative of the remaining seven animals.

Immunolabelling for vglut-1 and Cx36 in all vestibular nuclear subdivisions on the intact side of animals taken for labyrinthectomy was not discernibly different from that seen in unoperated animals. This allow animals to serve as their own controls for quality of tissue fixation and immunolabelling; thus, comparisons in Figure 11 show labelling on the control left side *vs.* lesioned right side. As shown at low magnification in a field of LVN and MVN, vglut-1-positive terminals normally associated with neuronal somata and their initial dendrites on the control side (Fig. 11A) were largely absent on the lesioned side (Fig. 11B). This was accompanied by an equally large loss of labelling for Cx36, as shown in the LVN by comparison of the intact (Fig. 11C) *vs.* lesioned (Fig. 11D) side. Similar depletions of vglut-1 around neuronal somata were seen in the SpVN, as shown at low magnification of the control (Fig. 11E) *vs.* lesioned side (Fig. 11F). In Fig. 11G and H, higher magnifications of the boxed areas in Fig. 11E and F show comparisons of labelling for vglut-1 in relation that of Cx36 on the intact *vs.* lesioned side of the SpVN. Figures 11G1 and G2 show the same field on the intact side, and Figures 11H1 and H2 show the same field on the lesioned side. The insets with blue counterstaining show the localization of neurons in these fields. The Cx36-puncta that were typically associated with vglut-1-positive terminals on the intact side (Fig. 11H) were largely depleted along with these terminals on the lesioned side, and what remained was a sparse scattering of vglut-1 terminals and Cx36-puncta (Fig. 11G). Higher magnifications of the boxed areas in Fig. 11G and Fig. 11H are shown in Fig. 11I and 11J, respectively. Compared with the relatively large size of the vglut-1-positive terminals (Fig. 11I1) and clusters of Cx36-puncta (Fig. 11I2) normally seen on somata in vestibular nuclei on the intact side, the remaining terminals on the lesion side tended to be smaller and less often associated with somata (Fig. 11J1), and clusters of Cx36-puncta were also diminished in size (Fig. 11J2). The few small terminals that remained associated with neuronal somata maintained co-localization with Cx36-puncta, as shown in the inset in Fig. 11J2, representing overlay of the boxed areas in Fig. 11J1 and J2. A similar loss in labelling for vglut-1 terminals and Cx36-puncta was seen in the SuVN on the intact *vs.* lesioned side (not shown).

Our results are in contrast to a previous report, where unilateral labyrinthectomy in rats failed to reduce labelling of Cx36 in vestibular nuclei, and where the pattern of labelling observed in these nuclei in normal animals had a somewhat different appearance than presented here (Beraneck et al., 2009), possibly due to use of different fixation conditions under which specificity of their immunolabelling was not tested. These same investigators reported significant effects of gap junction blockers on the electrophysiological properties of vestibular neurons in guiniea pig where, as noted in above, we found an absence of labelling for Cx36.

DISCUSSION

The present results extend previous reports on neuronal gap junctions and mixed synapses in rodent vestibular nuclei. These junctions are almost certainly composed of Cx36, and many of their features, deduced from the more global view afforded by immunofluorescence labelling of Cx36, are consistent with those derived from earlier detailed ultrastructural observations. Their size was reported to range from 0.05-0.5 μm (Sotelo and Palay 1970), roughly matching the 0.65 μm average size of Cx36-puncta measured here, if taking into

account that these puncta appear somewhat larger due to fluorescence light dispersion (halation). The localization of Cx36-puncta to nerve terminals, in this case those labelled for vglut-1, is also consistent with descriptions of mixed synapses in vestibular nuclei. Individual nerve terminals in these nuclei were reported to form more than one gap junction with a postsynaptic element (Sotelo and Palay, 1970), corresponding to multiple Cx36-puncta we found at the majority of terminals. Typically, terminals forming gap junctions in rat LVN were described as being relatively large, ranging 2–4 μm in diameter (Sotelo and Palay, 1970; Karhunen, 1973), similar to the on average 3 μm diameter boutons at which Cx36-puncta were localized. A class of long slender axon terminals were also described in the LVN (Sotelo and Palay, 1970), which likely correspond to the long vglut-1-positive profiles bearing Cx36-puncta described here.

Neuronal somata contacted by large terminals were reported to be among the largest in the LVN, and included large ventrally located Deiters neurons, with on average 60% of their parykaryal surface covered by these boutons (Sotelo and Palay, 1970). Our results show Cx36 co-localization with large vglut-1-positive terminals ending on among the largest neurons in each of the vestibular subdivisions, although those in the SuVN tended to be more on the medium size. Mixed synapses in the LVN were reported to be present mainly on neuronal somata or initial dendrite segments (Sotelo and Palay, 1970; Korn et al 1973), consistent with locations displaying the greatest concentrations of Cx36-puncta. Dendro-dendritic, dendro-somatic and soma-somatic gap junctions were reported to be absent in the LVN of adult rat (Sotelo and Palay, 1970; Korn et al., 1973), which is supported by present results showing that nearly all Cx36-puncta in vestibular nuclei of adult rodent are associated with vglut-1-positive nerve terminals. Only very rarely did we find these Cx36-puncta at closely apposed small neuronal somata, but even these puncta may represent false-negative terminal association, because confocal through focus analysis often showed them to be associated with vglut-1-positive terminals located out of the plane of focus, which was not uncommon given that Cx36-puncta occur on the surface rather than within terminals.

Distribution of mixed synapses in vestibular nuclei

Mixed synapses were described in the LVN and the SpVN of rat (Sotelo and Palay, 1970; Korn et al., 1973; Sotelo and Korn, 1978) and the LVN of mouse (cited as unpublished observations in Sotelo and Korn, 1978). Present results now show that all four of the "classically" defined vestibular nuclei in both rat and mouse contain mixed synapses, *i.e.*, Cx36-puncta associated with vglut-1-positive terminals. While borders between these nuclei are often difficult to delineate, this is less of a concern here because immunolabelling for Cx36 differed little in regions where borders are indistinct. Several satellite cell groups included in the vestibular nuclear complex (e.g., groups y, e, x, z) were not examined here, but may be considered at a later date. Of note is the dorsocaudal portion of the LVN (dLVN), in which there was a near total absence of Cx36-puncta. The dLVN is populated by numerous "giant" neurons of Deiter (Shamboul, 1979; Mehler and Rubertone, 1985), but unlike other areas of the vestibular nuclear complex, it lacks or receives only sparse primary afferent input (reviewed in Barmack, 2003; Highstein and Holstein, 2006). The dLVN was presently found to be nearly devoid of the large 3 μm diameter vglut-1-positive terminals with which Cx36 was associated in other areas of the vestibular complex, but contained instead an abundance of much smaller vglut-1-positive terminals (~ 1 μm diameter) that were not labelled for Cx36.

Regarding species differences in observations of mixed synapses in mammalian vestibular nuclei, in their discussion of an ultrastructural study by Mugnaini et al. (1967) who did not describe gap junctions in cat LVN, Sotelo and Korn (1970) noted that large axon terminals appear to be absent in feline LVN, explaining in their view the concomitant absence of terminal-associated gap junctions. Our examination of the LVN in cat revealed the presence

of abundant large vglut-1-positive terminals (not shown) having a similar size range (*i.e.*, ~ 3.4 ± 0.23 μm) as those in rat LVN, consistent with observations of degenerating large terminals after transection of the vestibular nerve (Mugnaini et al., 1967). However, this structure as well as the other three major vestibular nuclear subdivisions in both cat and guinea pig were devoid of labelling for Cx36, which is consistent with the reported absence of electrical coupling between LVN neurons in the cat (Ito et al., 1964, 1969).

Development of mixed synapses in vestibular nuclei

Developmental studies of mixed synapses in the vestibular nuclei are rare, except in the chick tangential nucleus (avian vestibular equivalent), where these are formed by large callosal primary afferent fibers that terminate as spoon endings on principal neurons (Hinojosa and Robertson, 1967). In this nucleus, abundant mixed synapses are present at late embryonic stages and continue to increase after hatching and towards adulthood (Peusner, 1981, 1984), but this system has resisted demonstrations of electrical coupling and has yielded variable results in studies of dye-coupling (Peusner and Giaume, 1994; Arabshahi et al., 1997; Shao et al., 2008). Our findings in rat that mixed synapses in the vestibular nuclei emerge in small numbers shortly after birth, that their maturation is somewhat protracted, reaching an adult appearance only at about the third postnatal week, and that this occurs slightly earlier in the SpVN, parallels the same period of time over which there is gradual maturation of the connections and functions of these nuclei in the control of posture, balance and gaze (Clarac, 1998).

The many Cx36-puncta that were not associated with vglut-1 at earlier ages could reflect: 1. Localization on terminals with immunohistochemically undetectable levels of vglut-1. This is possible because large terminals in LVN do not reach their adult size or abundance of vesicles till about postnatal day ten (Karhunen, 1973); 2. Localization on neurons that await their full complement of large terminal contacts to which Cx36 relocates for mixed synapse formation. This is unlikely because the number of large terminals on large LVN neurons changes little during postnatal development (Karhunen, 1973); or 3. Purely electrical synapses (*i.e.*, not mixed synapses) that are formed between dendrites, neuronal somata or dendrites and somata, and that gradually diminish in number, as occurs during development in other regions of the CNS (Bruzzone and Dermietzel, 2006; Meier and Dermietzel, 2006). This latter point is likely, but all three of these issues remain to be addressed by ultrastructural studies.

Source of vestibular afferents forming mixed synapses

The anatomical source of terminals forming mixed synapses in rodent vestibular nuclei has been a point of uncertainty ever since the identification of these synapes over four decades ago. Korn et al. (1973) noted that various lesions, including vestibular nerve section, failed to produce degeneration of large terminals bearing gap junctions, apparently excluding a primary afferent origin. However, there is evidence in rat for electrical transmission by primary vestibular fibers to vestibular neurons (Wylie, 1973). Moreover, electrical transmission by eighth nerve afferents has been described in toadfish (Korn et al., 1977), frog (Precht et al., 1974; Babalian and Shapovalov, 1984), lizard (Richter et al., 1975) and pigeon (Wilson and Wylie, 1970). Based on these findings, together with observations in some of these systems that typically the largest primary vestibular afferent terminals form mixed synapses, it seems to have been inferred that the large terminals forming these synapses in rat vestibular nuclei are of primary afferent origin (Korn et al., 1977; Sotelo, 1975; Sotelo and Korn, 1978; Sotelo and Triller, 1981). More recently, unilateral ablation of Scarpa's ganglion, housing the somata of vestibular primary afferents, was demonstrated to cause a substantial loss of vglut-1-containing terminals in deafferented vestibular nuclei (Zhang et al., 2011). A similar result obtained here after labyrinthectomy is consistent with

evidence suggesting the glutamatergic nature of vestibular primary afferents (Highstein and Holstein, 2006), and indicates that *large* vglut-1-containing terminals in the vestibular nuclei originate from primary afferents. The accompanying loss of Cx36-puncta revealed association of Cx36-containing gap junctions with terminals of these afferents. It remains unclear why Korn et al. (1973) failed to find degeneration of large nerve terminals bearing gap junctions after vestibular nerve lesions.

Vestibular neuronal coupling via presynaptic axons

Previously described electrical coupling between rat LVN neurons was concluded to be mediated by presynaptic fibers (Korn et al., 1973), where collaterals of a single fiber innervate and form mixed synapses on two different neurons, allowing activity in one neuron to be transmitted to another via the gap junctions at each end of the collateral. There is ample precedent for mediation of neuronal coupling by presynaptic fibers in lower vertebrates (Pappas and Bennett, 1966; Bennett et al., 1967; Kriebel et al., 1969; Korn et al., 1977). The inferred occurrence of this process in rat LVN neurons is based on fulfillment of several criteria: 1. Ultrastructural documentation of the presence of terminals forming mixed synapses on neurons (Sotelo and Palay, 1970; Korn et al., 1973); 2. Morphological support for the lack of gap junctions directly linking the neurons themselves (Korn et al, 1973), notwithstanding difficulties in proving their total absence; 3. Evidence for electrical transmission by fibers innervating neurons (Wylie, 1973); and 4. Anatomical data indicating that primary afferent fibers collateralize, providing the opportunity for collaterals to form contacts on separate neurons, for which there is ample evidence throughout the vestibular complex in cat (Sato et al., 1989; Imagawa et al., 1995, 1998), and which is unlikely to differ in rodent. These criteria have also been met to various degrees in a variety of non-mammalian species in which electrical coupling in the LVN or its anatomical counterpart has been observed (referenced in Korn et al., 1977; Sotelo and Korn, 1978), suggesting a phylogenetically conserved contribution of neuronal coupling in the LVN by way of presynaptic fibers.

Functional significance of morphologically mixed synapses

Various functions of gap junctions at mixed synapses in the vestibular nuclei have been considered (Korn et al., 1973; Sotelo and Korn, 1978), among which is the speed advantage of electrical over chemical transmission, with whatever attendant functional benefits this would have for secondary integrative processes within, and upstream of, the vestibular nuclei. While the importance of faster electrical transmission is understood in many electrically coupled systems in cold-blooded species, it has been repeatedly emphasized that there is little such advantage in mammals, where body temperature shortens chemical synaptic delay to speeds sometimes approaching or overlapping that of electrical synapses (Bennett, 1972, 1977, 1997, 2000; Bennett and Goodenough, 1978; see however Ostojic et al., 2009). Even with a shorter latency of transmission at electrical synapses, it has been noted that speed of motor responses triggered by vestibular activity would be more limited by physical constraints of movement imposed by body size (Korn et al., 1977).

If not for a transmission speed advantage or only minimally so, at least in mammals, an alternative consideration for the presence of mixed synapses is the provision of vestibular neuronal synchronous activity mediated by presynaptic fibers (Korn et al., 1977). The functional importance of such synchrony is well understood in some coupled systems of lower vertebrates (Bennett, 1974, 1977; Bennett and Goodenough, 1978), and more recently is becoming recognized in a variety of structures in mammalian brain (Bennett and, Zukin, 2004; Connors and Long, 2004; Hormuzdi et al., 2004). It might also be considered that in a system with highly collateralized primary afferents, such as the vestibular nuclear complex, coupling of postsynaptic neurons via presynaptic fibers could promote synchronous

responses specifically in ensembles of target neurons receiving a functionally common afferent input from an end organ receptor. One can imagine that this would be an efficient means to temporally network the output strength of a set of vestibular neurons in response to a specific sensory input. This does not explain, however, the presumptive requirement for mixed synapse-mediated synchrony among vestibular nuclei in a series of species ranging from lower vertebrates up to and including rodents, but not in cat or guinea pig which appear to lack mixed synapses in the vestibular nuclei.

A possibility for mixed synapses at vestibular afferents not yet considered involves the macromechanics of the semicircular canals, in particular canal size in relation to their sensitivity for signal generation in response to head rotation. Canal size increases with body mass; specifically, the radius of curvature (R) and cross-sectional area (r) of the canal ducts are key parameters, where Rr^2 is predicted to determine canal sensitivity to movement and, consequently, range of vestibular afferent nerve activity. In vertebrates, Rr^2 varies 20-fold over a wide range of body mass (Jones and Spells, 1963; Howland and Masci, 1973; reviewed in Goldberg et al., 2012), and there is evidence in mammals that semicircular canal size strongly correlates with vestibular nerve afferent sensitivity (Yang and Hullar, 2007; see also Goldberg et al., 2012). Canal sizes in mice and rats, as well as in lower vertebrates of small body mass, may have reached a lower limit insufficient to support vestibular afferent nerve activity required for maintenance of vestibular functions. In this event, perhaps we need look no further for a possible role of an electrical component at vestibular afferents than to consider this component as a mechanism that has been conserved (or added) to compensate for lower vestibular afferent activity from smaller semicircular canals, *i.e.*, the possibility of dual chemical and electrical transmission, if this occurs at vestibular primary afferents, may be more effective than chemical alone in generating adequate postsynaptic responses. This does not negate a possible role of electrical coupling between vestibular neurons mediated by presynaptic fibers, which may represent an additional compensatory mechanism to augment vestibular primary afferent input.

It should be noted that while a very small percentage of open gap junction channels in relatively large or numerous junctional plaques linking neurons can support electrical coupling (*e.g.*, Curti et al., 2012), it cannot be a forgone conclusion that sufficient numbers of open channels occur in gap junctional plaques of vestibular afferent terminals to confer robust electrical coupling. Further consideration of the above possibilities must, therefore, await not only more detailed electrophysiological demonstrations of a functional electrical component at the morphologically mixed synapses in the vestibular complex, but also evidence for operative dual chemical and electrical components at individual mixed synapses.

Supplementary Material

Refer to Web version on PubMed Central for supplementary material.

Acknowledgments

This work was supported by grants from the Canadian Institutes of Health Research and from the National Science and Engineering Council to J.I.N., and by grants from the National Institutes of Health (NS31027, NS44010, NS44395) to J.E. Rash with subaward to J.I.N. We thank B. McLean for excellent technical assistance, and Dr. D. Paul (Harvard University) for providing breeding pairs of Cx36 knockout mice and their wild-type counterparts.

Abbreviations

CNS	Central nervous system

Cx36	connexin36
ko	knockout
LVN	lateral vestibular nucleus
MVN	medial vestibular nucleus
MVNmc	medial vestibular nucleus magnocellular part
MVNpc	medial vestibular nucleus parvicellular part
PBS	phosphate-buffered saline
SpVN	spinal vestibular nucleus
SuVN	superior vestibular nucleus
TBS	50 mM Tris-HCl, pH 7.4, 1.5% NaCl
TBSTr	TBS containing 0.3% Triton X-100
vglut-1	vesicular glutamate transporter-1

REFERENCES

Arabshahi A, Giaume C, Peusner KD. Lack of biocytin transfer at gap junctions in the chicken vestibular nuclei. Int J Devel Neurosci. 1997; 15:343–352. [PubMed: 9253658]

Babalian AL, Shapovalov AI. Mode of synaptic transmission between vestibular afferents and neurons of the vestibular nucleus in the frog. Brain Res. 1984; 309:163–167. [PubMed: 6091845]

Barmack NH. Central vestibular system: vestibular nuclei and posterior cerebellum. Brain Res Bull. 2003; 60:511–541. [PubMed: 12787870]

Bautista W, Nagy JI, Dai Y, McCrea DA. Requirement of neuronal connexin36 in processes mediating presynaptic inhibition of low threshold afferents in functionally mature motor systems of mouse spinal cord. J Physiol. 2012; 590:3821–3839. [PubMed: 22615430]

Bautista W, McCrea DA, Nagy JI. Connexin36 forms purely electrical synapses in sexually dimorphic lumbosacral motor nuclei in spinal cord of developing and adult rat and mouse. Submitted. 2013

Bennett MVL. Physiology of electrotonic junctions. Ann NY Acad Sci. 1966; 137:509–539. [PubMed: 5229812]

Bennett MVL, Pappas G, Gimenez M, Nakajima Y. Physiology and ultrastructure of electrotonic junctions - IV. Medullary electromotor nuclei in gymnotid fish. J Neurophysiol. 1967; 30:236–300. [PubMed: 6045196]

Bennett, MVL. A comparison of electrically and chemically mediated transmission. In: Pappas, GD.; Purpura, DP., editors. Structure and Function of Synapses. NY: Raven; 1972. p. 221-256.

Bennett, MVL. Flexibility and rigidity in electrotonically coupled systems. In: Bennett, MVL., editor. Synaptic Transmission and Neuronal Interaction. NY: Raven; 1974. p. 153-178.

Bennett, MVL. Electrical transmission: a functional analysis and comparison with chemical transmission. In: Kandel, ER., editor. Cellular Biology of Neurons, vol I, sec. I, The Handbook of Physiology – The Nervous System I. Baltimore: Williams and Wilkins; 1977. p. 357-416.

Bennett MVL, Goodenough DA. Gap junctions, electrotonic coupling, and intercellular communication. Neurosci Res Pro Bull. 1978; 16:373–485.

Bennett MVL. Gap junctions as electrical synapses. J Neurocytol. 1997; 26:349–366. [PubMed: 9278865]

Bennett MVL. Electrical synapses, a personal perspective (or history). Brain Res Rev. 2000; 32:16–29. [PubMed: 10751654]

Bennett MVL, Zukin SR. Electrical coupling and neuronal synchronization in the mammalian brain. Neuron. 2004; 41:495–511. [PubMed: 14980200]

Beraneck M, Uno A, Vassias I, Idoux E, De Waele C, Vidal P-P, Vibert N. Evidence against a role of gap junctions in vestibular compensation. Neurosci Lett. 2009; 450:97–101. [PubMed: 19084577]

Brodal, A. Neurological anatomy. 3rd ed.. New York: Oxford University Press; 1981.

Bruzzone R, Dermietzel R. Structure and function of gap junctions in the developing brain. Cell Tiss Res. 2006; 326:239–248.

Clarac F, Vinay L, Cazalets J-R, Fady J-C, Jamon M. Role of gravity in the development of posture and locomotion in the neonatal rat. Brain Res Rev. 1998; 28:35–43. [PubMed: 9795120]

Condorelli DF, Parenti R, Spinella F, Salinaro AT, Belluardo N, Cardile V, Cicirata F. Cloning of a new gap junction gene (Cx36) highly expressed in mammalian brain neurons. Eur J Neurosci. 1998; 10:1202–1208. [PubMed: 9753189]

Condorelli DF, Belluardo N, Trovato-Salinaro A, Mudo G. Expression of Cx36 in mammalian neurons. Brain Res Rev. 2000; 32:72–85. [PubMed: 10751658]

Connors BW, Long MA. Electrical synapses in the mammalian brain. Annu Rev Neurosci. 2004; 27:393–418. [PubMed: 15217338]

Cowan, WM.; Kandel, ER. A brief history of synapses and synaptic transmission. In: Cowan, WM.; Sudhof, TC.; Stevens, CF., editors. Synapses. Baltimore: Johns Hopkins University Press; 2001. p. 1-88.

Curti S, Hoge G, Nagy JI, Pereda AE. Synergy between electrical coupling and membrane properties promotes strong synchronization of neurons of the mesencephalic trigeminal nucleus. J Neurosci. 2012; 32:4341–4359. [PubMed: 22457486]

Furshpan EJ. Electrical transmission at an excitatory synapse in a vertebrate brain. Science. 1964; 144:878–880. [PubMed: 14149407]

Goldberg, JM.; Wilson, VJ.; Cullen, KE.; Angelaki, DE.; Broussard, DM.; Buttner-Ennever, JA.; Fukushima, K.; Minor, LB. The Vestibular System; A Sixth Sense. NY: Oxford Univ Press; 2012.

Hamzei-Sichani F, Davidson KGV, Yasumura T, Janssen WGM, Wearne SL, Hof PR, Traub RD, Gutierrez R, Ottersen OP, Rash JE. Mixed electrical-chemical synapses in adult rat hippocampus are primarily glutamatergic and coupled by connexin-36. Front Neuroanat. 2012; 6:1–26. [PubMed: 22291620]

Highstein SM, Holstein GR. The anatomy of the vestibular nuclei. Prog Brain Res. 2006; 151:157–203. [PubMed: 16221589]

Hinojosa R, Robertson JD. Ultrastructure of the spoon type synaptic endings in the nucleus vestibularis tangentialis of the chick. J Cell Biol. 1967; 34:421–430. [PubMed: 5340758]

Hinojosa R. Synaptic ultrastructure in the tangential nucleus of the goldfish (*Carassius auratus*). Am J Anat. 1973; 137:159–186. [PubMed: 4574401]

Hoge GJ, Davidson KGV, Yasumura T, Castillo PE, Rash JE, Pereda A. The extent and strength of electrical coupling between inferior olivary neurons is heterogeneous. J Neurophysiol. 2010; 105:1089–1101. [PubMed: 21177999]

Hormuzdi SG, Filippov MA, Mitropoulon G, Monyer H, Bruzzone R. Electrical synapses: a dynamic signaling system that shapes the activity of neuronal networks. Biochem Biophys Acta. 2004; 1662:113–137. [PubMed: 15033583]

Howland HC, Masci J. The Phylogenetic allometry of the semicurcular canals of small fishes. Z Morph Tiere. 1973; 75:283–296.

Imagawa M, Isu N, Sasaki M, Endo K, Ikegami H, Uchino Y. Axonal projections of utricular afferents to the vestibular nuclei and the abducens nucleus in cats. Neurosci Lett. 1995; 186:87–90. [PubMed: 7777205]

Imagawa M, Graf W, Sato H, Suwa H, Isu N, Izumi R, Uchino Y. Morphology of single afferents of the saccular macula in cats. Neurosci lett. 1998; 240:127–130. [PubMed: 9502220]

Ito M, Hongo T, Yoshida M, Okada Y, Obata K. Antidromic and transsynaptic activation of Deiters neurons induced from the spinal cord. Jap J Physiol. 1964; 14:638–658. [PubMed: 14252836]

Ito M, Hongo T, Okada Y. Vestibular-evoked postsynaptic potentials in Deiters' neurons. Exp Brain Res. 1969; 7:214–230. [PubMed: 5795248]

Jones GM, Spells KE. A theoretical and comparative study of the functional dependence of the semicircular canal upon its physical dimensions. Proc R Soc Lond. 1963; 157:403–419. [PubMed: 14041997]

Kamasawa N, Furman CS, Davidson KGV, Sampson JA, Magnie AR, Gebhardt BR, Kamasawa M, Yasumura T, Zumbrunnen JR, Pickard GE, Nagy JI, Rash JE. Abundance and ultrastructural diversity of neuronal gap junctions in the OFF and ON sublaminae of the inner plexiform layer of rat and mouse retina. Neuroscience. 2006; 142:1093–1117. [PubMed: 17010526]

Karhunen E. Postnatal development of the lateral vestibular nucleus (Deiters' nucleus) of the rat. Acta Oto-Lyryngol Suppl. 1973; 313:1–87.

Korn H, Sotelo C, Crepel F. Electrotonic coupling between neurons in the lateral vestibular nucleus. Exp Brain Res. 1973; 16:255–275. [PubMed: 4346867]

Korn H, Sotelo C, Bennett MVL. The lateral vestibular nucleus of the toadfish *opsanus Tau:* ultrastructural and electrophysiological observations with special reference to electrotonic transmission. Neuroscience. 1977; 2:851–884.

Kriebel ME, Bennett MVL, Waxman SG, Pappas GD. Oculomotor neurons in fish: electrotonic coupling and multiple sites of impulse initiation. Science. 1969; 166:520–524. [PubMed: 4309628]

Li X, Olson C, Lu S, Kamasawa N, Yasumura T, Rash JE, Nagy JI. Neuronal connexin36 association with zonula occludens-1 protein (ZO-1) in mouse brain and interaction with the first PDZ domain of ZO-1. Eur J Neurosci. 2004; 19:2132–2146. [PubMed: 15090040]

Li X, Kamasawa N, Ciolofan C, Olson CO, Lu S, Davidson KGV, Yasumura T, Shigemoto R, Rash JE, Nagy JI. Connexin45-containing neuronal gap junctions in rodent retina also contain connexin36 in both apposing hemiplaques, forming bi-homotypic gap junctions, with scaffolding contributed by zonula occludens-1. J Neurosci. 2008; 28:9769–9789. [PubMed: 18815262]

Mehler, WR.; Rubertone, JA. Anatomy of the vestibular nucleus complex. In: Paxinos, G., editor. The rat nervous system, Vol 2, Hindbrain and spinal cord. San Diego: Academic Press; 1985. p. 185-219.

Meier C, Dermietzel R. Electrical synapses--gap junctions in the brain. Results Probl Cell Differ. 2006; 43:99–128. [PubMed: 17068969]

Mugnaini E, Walberg F, Brodal A. Mode of termination of primary vestibular fibres in the lateral vestibular nucleus. An experimental electron microscopical study in the cat. Exp Brain Res. 1967; 4:187–211. [PubMed: 5598825]

Mugnaini E, Walberg F, Hauglie-Hanssen E. Observations on the fine structure of the lateral vestibular nucleus (Deiters' nucleus) in the cat. Exp Brain Res. 1967; 4:146–186. [PubMed: 5598823]

Nagy, JI.; Dermietzel, R. Gap junctions and connexins in the mammalian central nervous system. In: Hertzberg, EL., editor. Advances in Molecular and Cell Biology. Vol. Vol. 30. New York: JAI Press Inc; 2000. p. 323-396.

Nagy JI, Dudek FE, Rash JE. Update on connexins and gap junctions in neurons and glia in the mammalian central nervous system. Brain Res Brain Res Rev. 2004; 47:191–215. [PubMed: 15572172]

Nagy JI. Evidence for connexin36 localization at hippocampal mossy fiber terminals suggesting mixed chemical/electrical transmission by granule cells. Brain Res. 2012 In Press.

Ostojic S, Brunel N, Hakim V. Synchronization properties of networks of electrically coupled neurons in the presence of noise and heterogeneities. J Comput Neurosci. 2009; 26:369–392. [PubMed: 19034642]

Pappas GD, Bennett MVL. Specialized junctions involved in electrical transmission between neurons. Ann NY Acad Sci. 1966; 137:495–508. [PubMed: 5229811]

Pereda A, O'Brian JO, Nagy JI, Bukauskas F, Davidson KGV, Yasumura T, Rash JE. Connexin35 mediates electrical transmission at mixed synapses on Mauthner cells. J Neurosci. 2003; 23:7489–7503. [PubMed: 12930787]

Pereda A, Rash JE, Nagy JI, Bennett MVL. Dynamics of electrical transmission at club endings on the Mauthner cells. Brain Res Rev. 2004; 47:227–244. [PubMed: 15572174]

Peusner KD. An ultrastructural study of the development of synaptic endings in the nucleus vestibularis tangentialis of the chick embryo. Neuroscience. 1981; 6:2335–2350. [PubMed: 7329550]

Peusner KD. The development of synapses and “spoon” synaptic terminal space in the tangential vestibular nucleus: a quantitative electron microscopic study. J Comp Neurol. 1984; 230:372–385. [PubMed: 6520239]

Peusner KD. The first developing “mixed” synapses between vestibular sensory neurons mediate glutamate chemical transmission. Neuroscience. 1994; 58:99–113. [PubMed: 7909147]

Precht W, Richter A, Ozawa S, Shimazu S. Intracellular study of frog’s vestibular neurons in relation to the labyrinth and spinal cord. Expl Brain Res. 1974; 19:377–393.

Rash JE, Dillman RK, Bilhartz BL, Duffy HS, Whalen LR, Yasumura T. Mixed synapses discovered and mapped throughout mammalian spinal cord. Proc Natl Acad Sci (USA). 1996; 93:4235–4239. [PubMed: 8633047]

Rash JE, Staines WA, Yasumura T, Pate D, Hudson CS, Stelmack GL, Nagy J. Immunogold evidence that neuronal gap junctions in adult rat brain and spinal cord contain connexin36 (Cx36) but not Cx32 or Cx43. Proc Natl Acad Sci (USA). 2000; 97:7573–7578. [PubMed: 10861019]

Rash JE, Yasumura T, Dudek FE, Nagy JI. Cell-specific expression of connexins, and evidence for restricted gap junctional coupling between glial cells and between neurons. J Neurosci. 2001; 21:1983–2000. [PubMed: 11245683]

Rash JE, Olson CO, Davidson KGV, Yasumura T, Kamasawa N, Nagy JI. Identification of connexin36 in gap junctions between neurons in rodent locus coeruleus. Neuroscience. 2007a; 147:938–956. [PubMed: 17601673]

Rash JE, Olson CO, Pouliot WA, Davidson KGV, Yasumura T, Furman CS, Royer S, Kamasawa N, Nagy JI, Dudek FE. Connexin36 vs connexin32, “miniature” neuronal gap junctions, and limited electrotonic coupling in rodent suprachiasmatic nucleus. Neuroscience. 2007b; 149:350–371. [PubMed: 17904757]

Richter A, Precht W, Ozawa S. Responses of neurons of lizard’s, lacerta viridis, vestibular nuclei to electrical stimulation of the ipsi and contralateral VIIIth nerves. Pflugers Arch. 1975; 355:85–94. [PubMed: 1171430]

Richter K, Langnaese K, Kreutz MR, Olias G, Zhai R, Scheich H, Garner CC, Gundelfinger ED. Presynaptic cytomatrix protein bassoon is localized at both excitatory and inhibitory synapses of rat brain. J Comp Neurol. 1999; 408:437–448. [PubMed: 10340516]

Sato F, Sasaki H, Ishizuka N, Sasaki S-I, Mannen H. Morphology of single primary vestibular afferents originating from the horizontal semicircular canal in the cat. J Comp Neurol. 1989; 290:423–439. [PubMed: 2592621]

Shamboul KM. The lateral vestibular nucleus of the rat, with a note on its dorsal extension into the cerebellum. J Anat. 1979; 129:107–116. [PubMed: 511757]

Shao M, Gottesman-Davis A, Popratiloff A, Peusner KD. Dye coupling in developing vestibular nuclei. J Neurosci Res. 2008; 86:832–844. [PubMed: 17941057]

Söhl G, Degen J, Teubner B, Willecke K. The murine gap junction gene connexin36 is highly expressed in mouse retina and regulated during brain development. FEBS Lett. 1998; 428:27–31. [PubMed: 9645468]

Söhl G, Maxeiner S, Willecke K. Expression and functions of neuronal gap junctions. Nat Rev Neurosci. 2005; 6:191–200. [PubMed: 15738956]

Sotelo, C. Morphological correlates of electrotonic coupling between neurons in mammalian nervous system. In: Santini, M., editor. Golgi Centennial Symposium. New York: Raven Press; 1975. p. 355-365.

Sotelo C, Palay SL. The fine structure of the lateral vestibular nucleus in the rat. II. Synaptic organization. Brain Res. 1970; 18:93–115. [PubMed: 4313893]

Sotelo C, Korn H. Morphological correlates of electrical and other interactions through low-resistance pathways between neurons of the vertebrate central nervous system. Int Rev Cytol. 1978; 5:67–107. [PubMed: 389866]

Sotelo, C. Morphological basis for electrical communication between neurons in the central nervous system of vertebrates. In: Szentagothai, J.; Hamori, J.; Vizi, ES., editors. Neuron Concept Today. Budapest: Akademiai Kiado; 1977. p. 17-26.

Sotelo, C.; Triller, A. Morphological correlates of electrical, chemical and dual modes of transmission. In: Stjarne, L.; Lagercrantz, L.; Hedqvist, H.; Wennmalm, A., editors. Chemical neurotransmission, 75 years. New York: Academic Press; 1981. p. 13-28.

Stefanelli A, Caravita S. Ultrastructural features of the synaptic complex of the vestibular nuclei of *Lampetra planeri* (Bloch). Z Zellforsch. 1970; 108:282–296. [PubMed: 5465936]

Vivar C, Traub RD, Gutierrez R. Mixed electrical-chemical transmission between hippocampal mossy fibers and pyramidal cells. Eur J Neurosci. 2012; 35:76–82. [PubMed: 22151275]

Wilson VJ, Wylie RM. A short latency labyrintine input to the vestibular nuclei in the pigeon. Science. 1970; 168:124–127. [PubMed: 5417052]

Wylie RM. Evidence of electrotonic transmission in the vestibular nuclei of the rat. Brain Res. 1973; 50:179–183. [PubMed: 4347844]

Zhang FX, Pang YW, Zhang MM, Zhang T, Dong YL, Lai CH, Shum DKY, Chan YS, Li JL, Li YQ. Expression of vesicular glutamate transporters in peripheral vestibular structures and vestibular nuclear complex of rat. Neuroscience. 2011; 173:179–189. [PubMed: 21081152]

Highlights

- Cx36 is abundant in the vestibular nuclei (VN) of rat and mouse
- Cx36 is localized to sites of contact between axon terminals and VN neurons
- Axon terminals displaying Cx36 in VN are of primary afferent origin
- Mixed synapses in the VN had a relatively late appearance developmentally

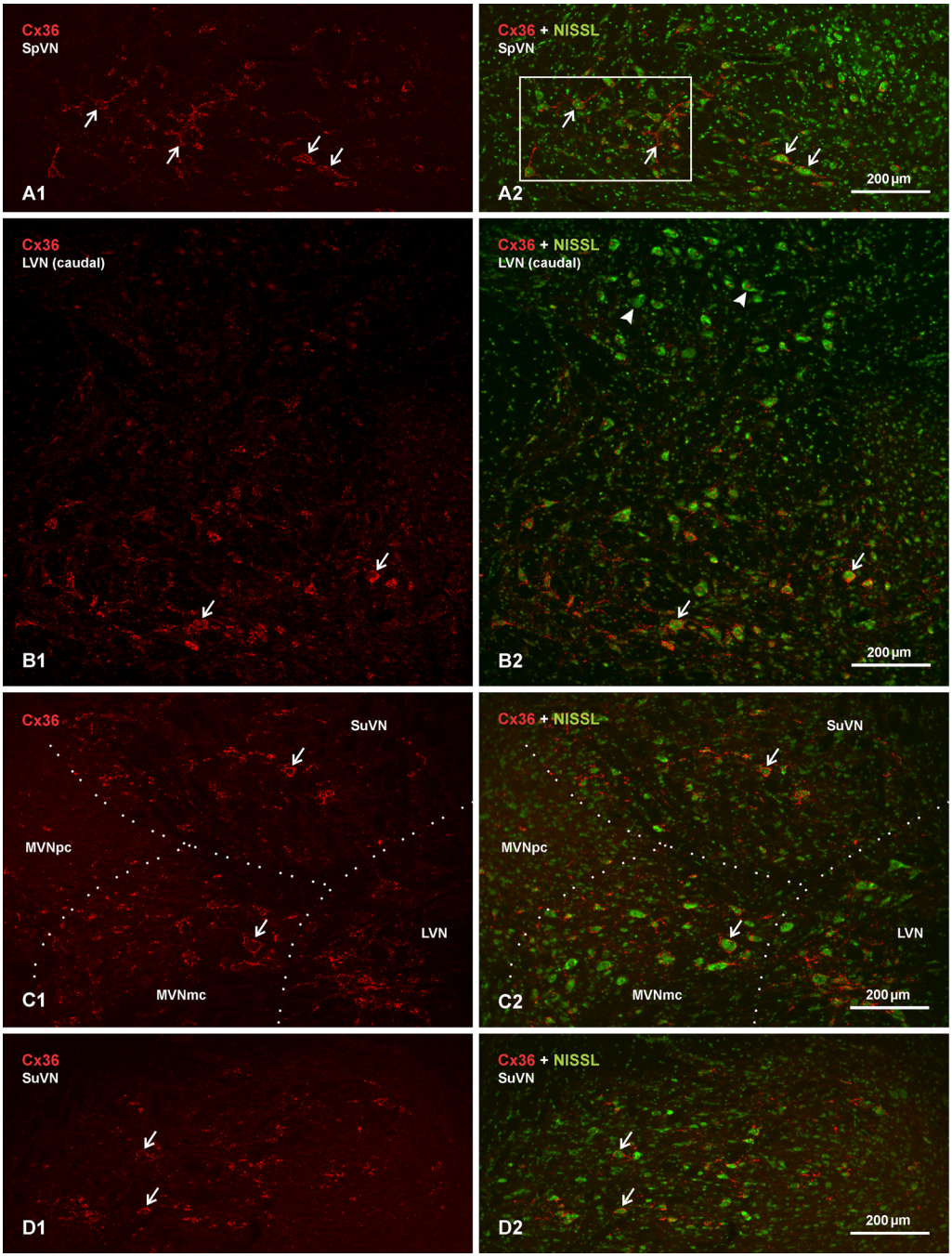

Fig. 1.

Low magnification images showing the distribution and density of immunofluorescence labelling for Cx36 in vestibular nuclei of adult rat. Images in the left column show labelling for Cx36 alone (red), and corresponding images in the right column show the same field, with red overlay on fluorescence Nissl counterstaining (green). (A1,A2) The caudal portion of the spinal vestibular nucleus (SpVN). (B1,B2) The caudal portion of the lateral vestibular nucleus (LVN). (C1,C2) The medial vestibular nucleus (MVN), mid-level of the LVN, and caudal portion of the superior vestibular nucleus (SuVN), with boundaries between nuclei shown by dotted lines. (D1,D2) The rostral portion of the SuVN. Labelling for Cx36 is densely distributed in most regions of the SpVN, the LVN and the MVN magnocellular part

(MVNmc), and moderately in the SuVN. Cx36 immunofluorescence is often associated with neuronal somata (arrows), diminishes in density towards the MVN parvicellular part (C2, MVNpc), and is mostly absent among a collection of large neuronal cell bodies (B2, arrowheads) in the dorsal half of the caudal LVN (B2, upper half of field shown).

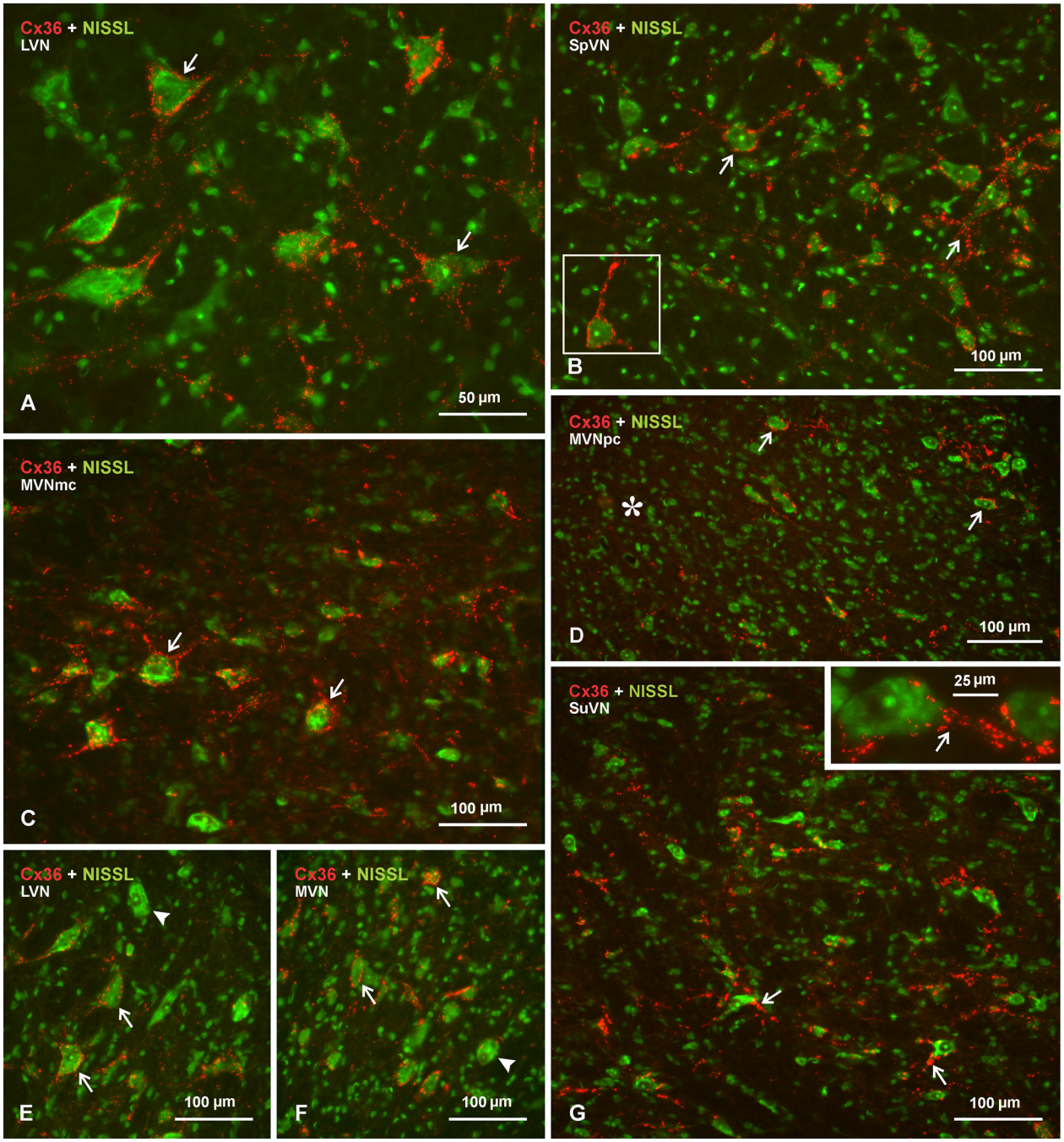

Fig. 2.

Higher magnification images showing the cellular localization of immunofluorescence labelling for Cx36 in vestibular nuclei of adult rat. All images are shown as overlay of labelling for Cx36 (red) with fluorescence Nissl counterstain (green). (A–C) Labelling of Cx36 is seen concentrated on, and decorating the surface of, large neuronal cell bodies and their initial dendrites (arrows) in LVN (A), SpVN (B, higher magnification of the boxed area shown in Fig. 1A2) and MVNmc (C). (D) Medial to large immunopositive neuronal somata in the MVNmc (arrows). Labelling is absent among small neurons in the MVNpc (asterisk). (E,F) Images showing heterogeneity of labelling around neuronal somata in LVN (E) and MVNmc (F), with some sparsely labelled or unlabelled large neurons (arrowheads)

intermingled with heavily labelled neurons (arrows). (G) Field in the SuVN showing Cx36 associated with small to medium sized neurons, where labelling is localized largely to neuronal initial dendrites (arrows), shown at higher magnification in inset.

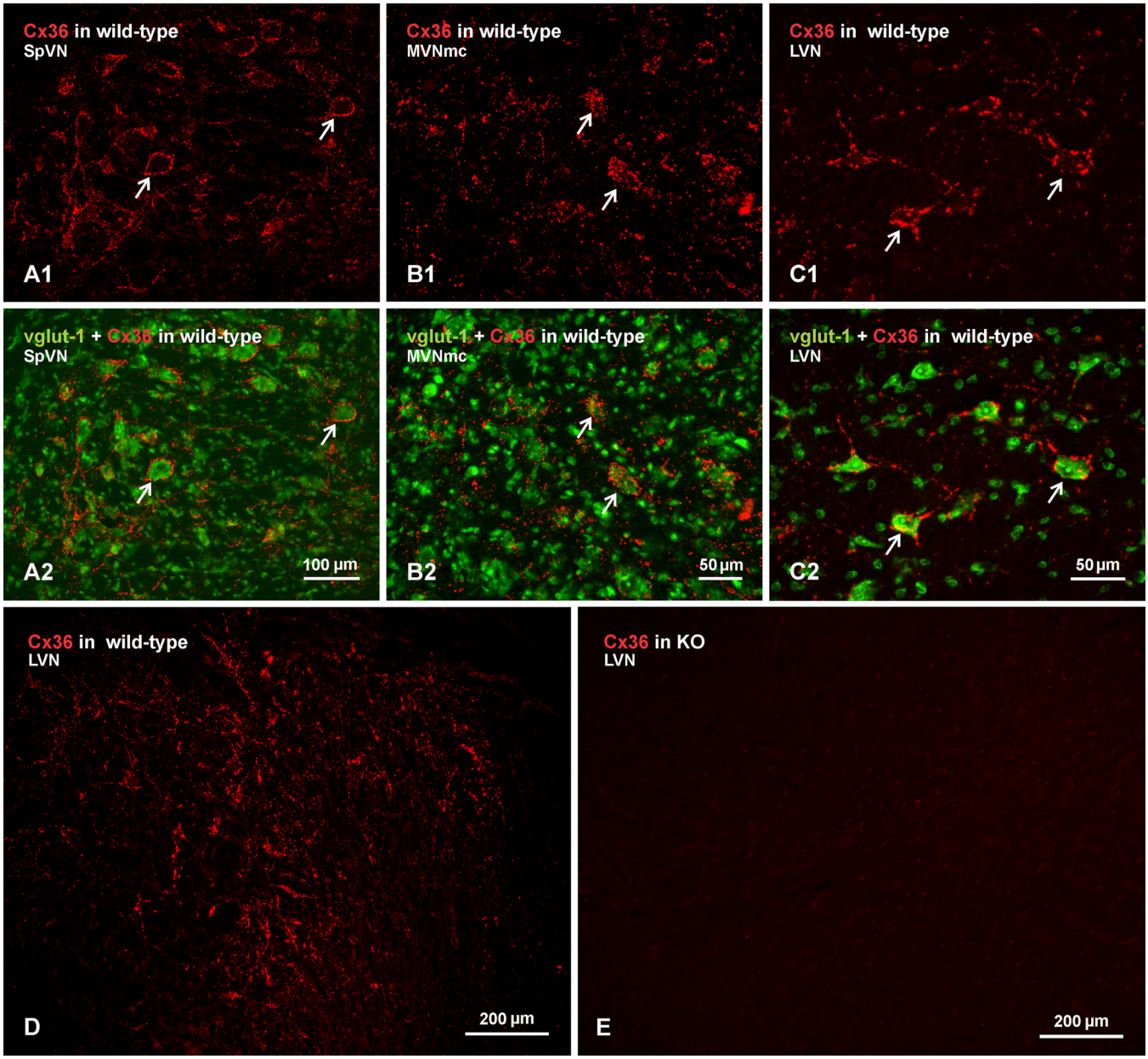

Fig. 3.

Immunofluorescence labelling of Cx36 in vestibular nuclei of wild-type adult mouse and absence of labelling in Cx36 knockout mouse. (A–C) The SpVN (A), MVNmc (B) and LVN (C), showing intense labelling of Cx36 (A1, B1 and C1, arrows) around medium and large size neuronal cell bodies, as seen in overlay with Nissl fluorescence counterstaining (green) of the corresponding fields (A2, B2, and C2, arrows). (D,E) Low magnification images showing Cx36 immunofluorescence in LVN of a wild-type mouse (D) and as similar field showing absence of labelling for Cx36 in the LVN of a Cx36 knockout mouse (E).

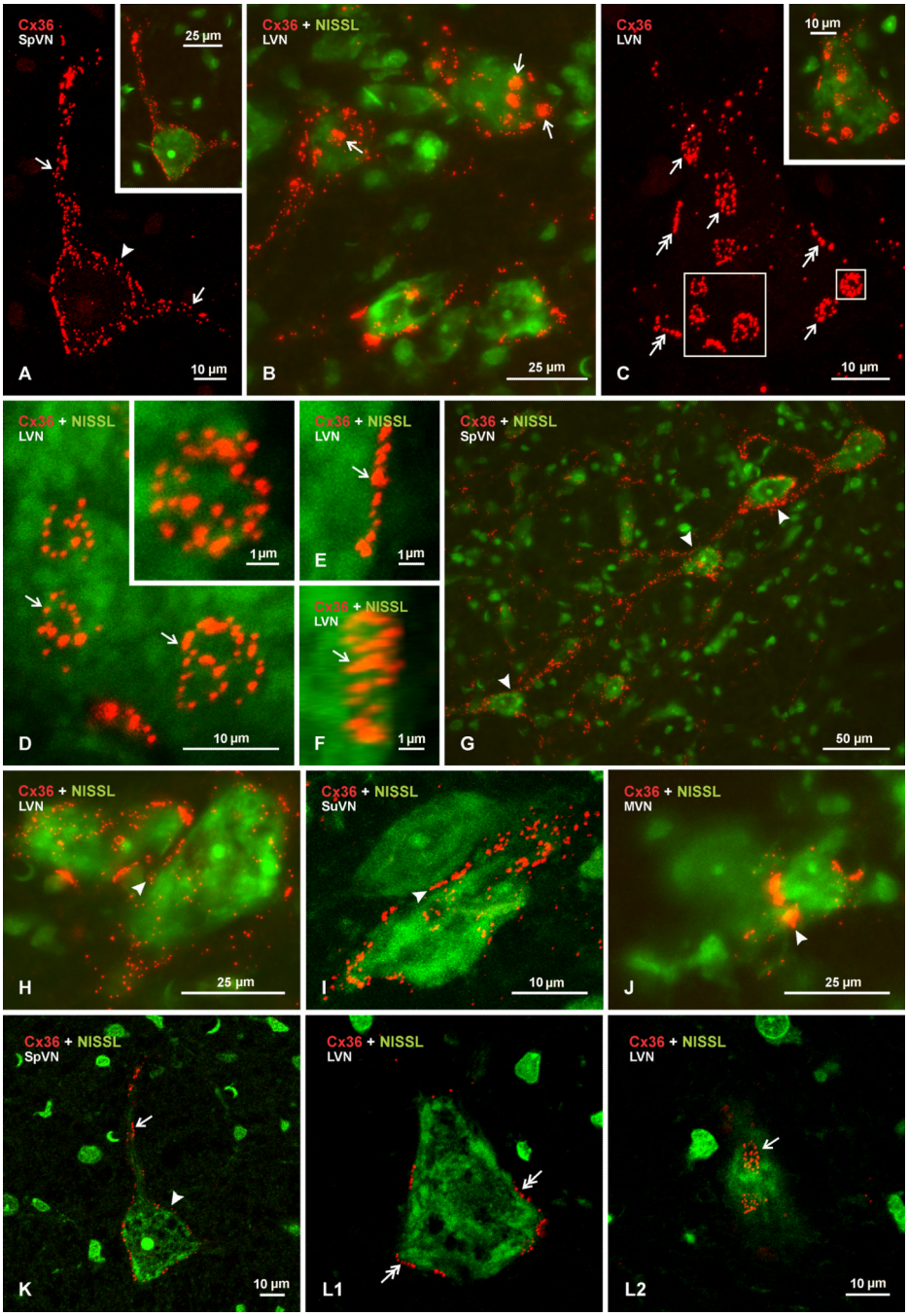

Fig. 4.

Laser scanning confocal images of Cx36 immunofluorescence associated with neurons in the vestibular nuclei of adult rat. Images are shown with labelling of Cx36 alone (red) or with Nissl fluorescence counterstaining (green) in overlay. (A) Image of the boxed area in Fig. 2B, showing Cx36 immunofluorescence on a single neuron in the SpVN, with Nissl fluorescence overlay of the same neuron in the inset. Labelling appears punctate and is seen throughout the soma surface (arrowhead) and along two large initial dendrites (arrows). (B) Confocal image of several neuronal somata in the LVN, displaying patches of dense labelling (arrows) as well as dispersed punctate labelling for Cx36 on their surface. (C) Higher magnification of a single neuron in the LVN, with Nissl counterstaining overlay in

inset, showing dense patches of labelling to consist of clusters of numerous Cx36-positive puncta (arrows). Also seen are linear arrangements of Cx36-puncta at the perimeter of neuronal somata (double arrows). (D–F) Confocal images showing individual clusters of Cx36-puncta (arrows) viewed *en face* (D, magnification of large boxed area in C), and in inset (D, magnification of the small box in C), with clusters consisting of different numbers and sizes of Cx36-puncta. (E,F) Image of a cluster of Cx36-puncta viewed on edge (E), and the same image (F) rotated by 30o in the horizontal axis to reveal the presence of a cluster of puncta. (G) Image of neurons in the SpVN with labelling for Cx36 along dendrites that appear to extend close to nearby neuronal somata (arrowheads). (H-J) Rare examples of Cx36-puncta (arrowheads) located between relatively small neurons in LVN (H), SuVN (I) and MVN (J). (K) Single scan image taken from Figure 4A, which was a z-stack of 13 scans, showing punctate immunofluorescence labelling of Cx36 (red) on the surface of the somata (arrowhead) and an initial dendrite (arrow) of a Nissl fluorescence counterstained neuron (green). (L) Single scan images taken from the image in Figure 4C (z-stack of 11 scans), showing a scan through the cell center with Cx36-puncta localized around the cell periphery (L1, double arrows), and a scan through the upper cell surface with Cx36-puncta localized at the cell surface (L2, arrow). The single scans show absence of intracellular labelling and localization of Cx36-puncta at the cell periphery.

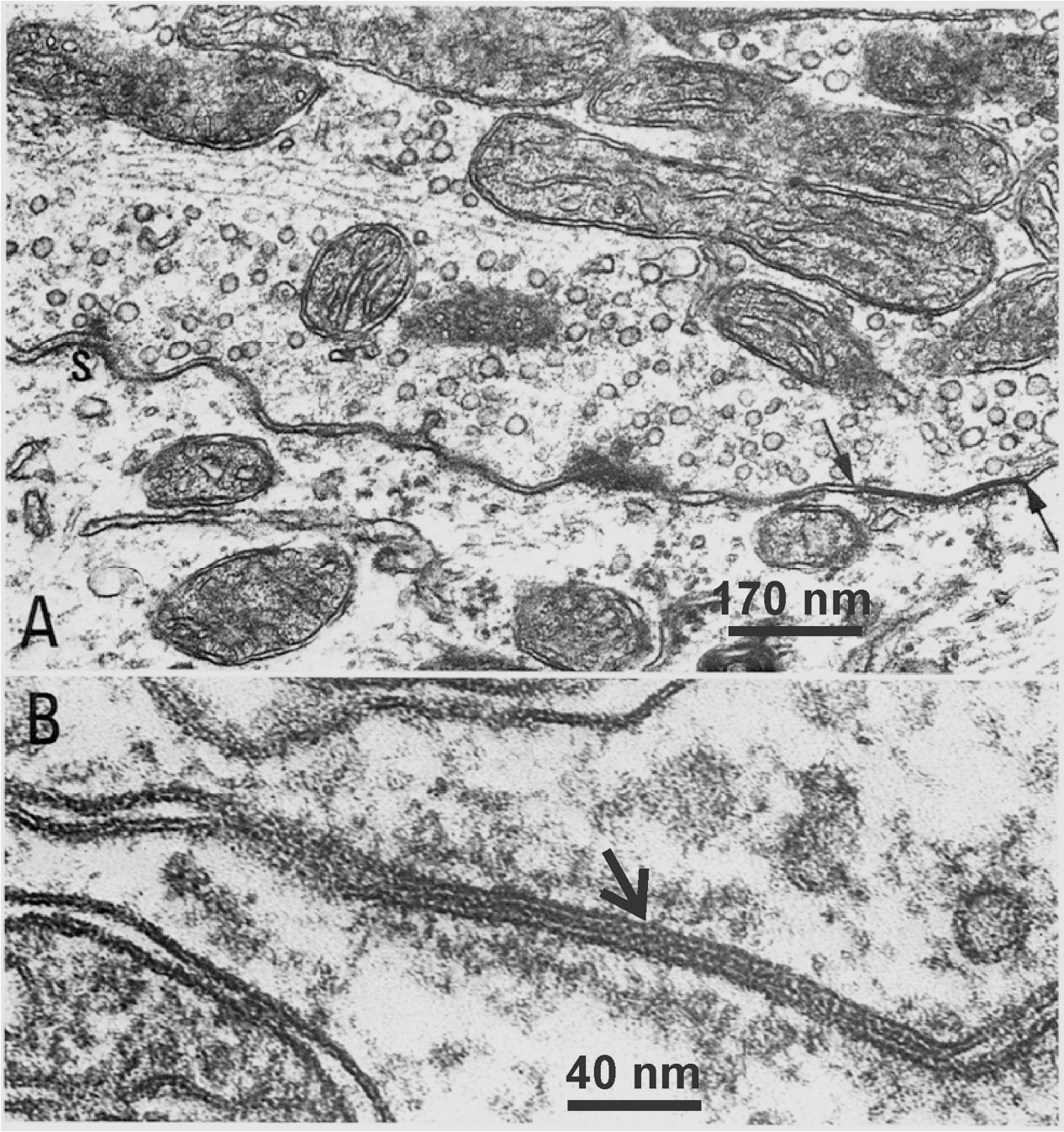

Fig. 5.

Reproduced from Korn et al. (1973), with permission from Springer-Science + Business Media, with scale bars added. Gap junctions in the LVN. (A) Electron micrograph of a large axon terminal synapsing on the perikaryon of a giant cell. Two types of junctional complexes are localized at this synaptic interface constituting a “mixed synapse”. At the left an “active” zone (S) with its associated dense projections and vesicles is shown. At the right the apposed plasma membranes converge into a “gap” junction (arrows). (B) High magnification of a “gap” junction between another large axon terminal and the perikaryon of another cell. There is a seven-layered structure of the junction and the layers of semidense cytoplasmic material undercoating the junction on each side.

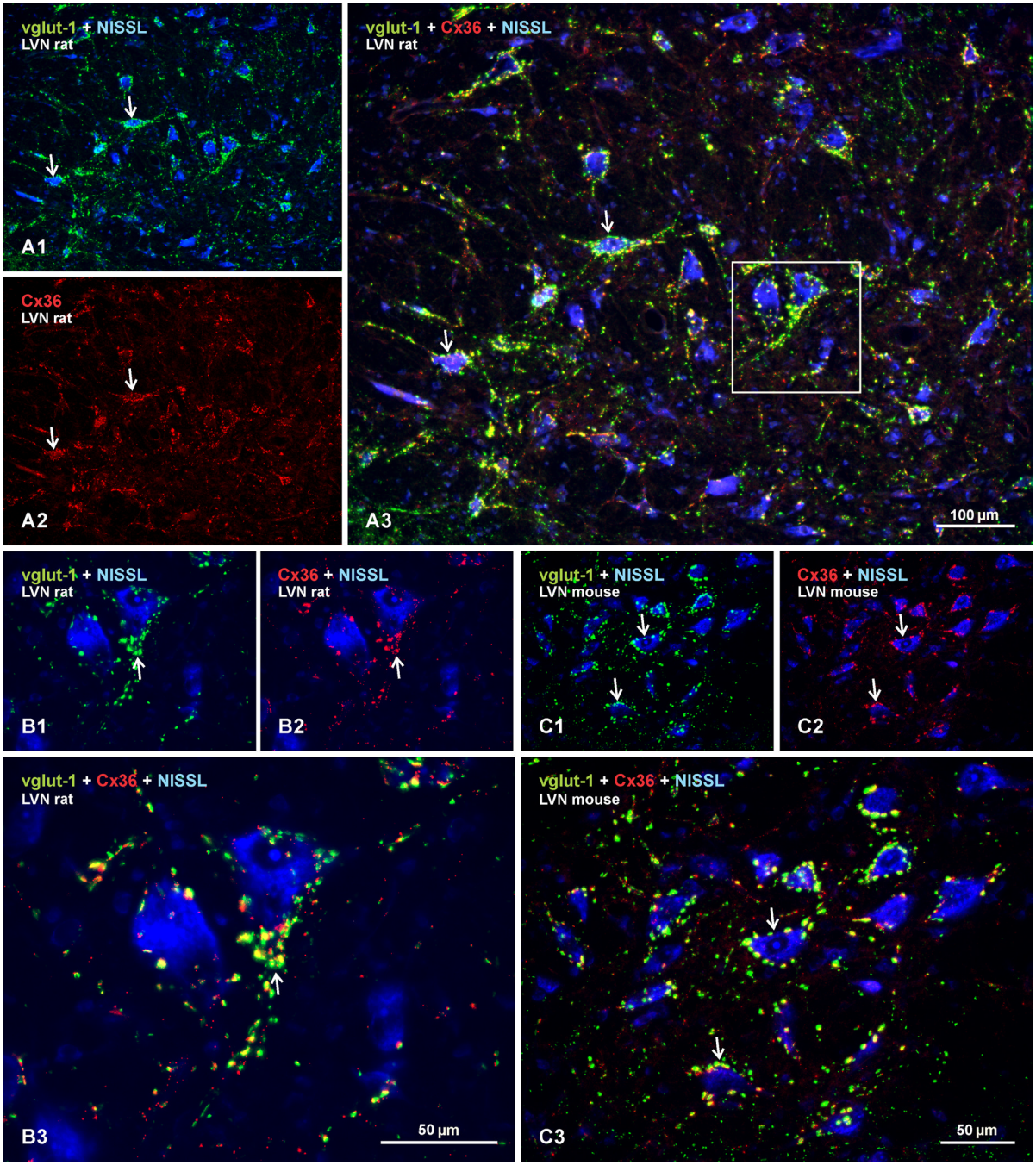

Fig. 6.

Double immunofluorescence labelling of Cx36 and vglut-1 in the LVN of adult rat and mouse. Sections were labelled for Cx36 (red), vglut-1 (green) and counterstained with Nissl fluorescence (blue). (A) Low magnification image of rat LVN, showing labelling for vglut-1 and Nissl fluorescence overlay (A1), and the same field showing labelling for Cx36 alone (A2), and overlay of all three colors (A3). Neuronal somata and their initial dendrites heavily invested with dense concentrations of vglut-1-positive nerve terminals (A1, arrows) are laden with Cx36-puncta (A2, arrows), with substantial Cx36/vglut-1 co-localization, as seen by yellow after red/green merge (A3, arrows). (B) Higher magnification of the boxed area in A3, showing vglut-1/Nissl overlay (B1), Cx36/Nissl overlay (B2), and merge of all

these labels (B3), where the majority of vglut-1-positive terminals are seen to display labelling for Cx36 (B3 arrow). (C) Mouse LVN, showing similar dense labelling of vglut-1 around neuronal somata (C1, arrows), with matching pattern of labelling for Cx36 (B2, arrows) and a high degree of Cx36/vglut-1 co-localization, as seen by yellow in overlay (C3, arrows).

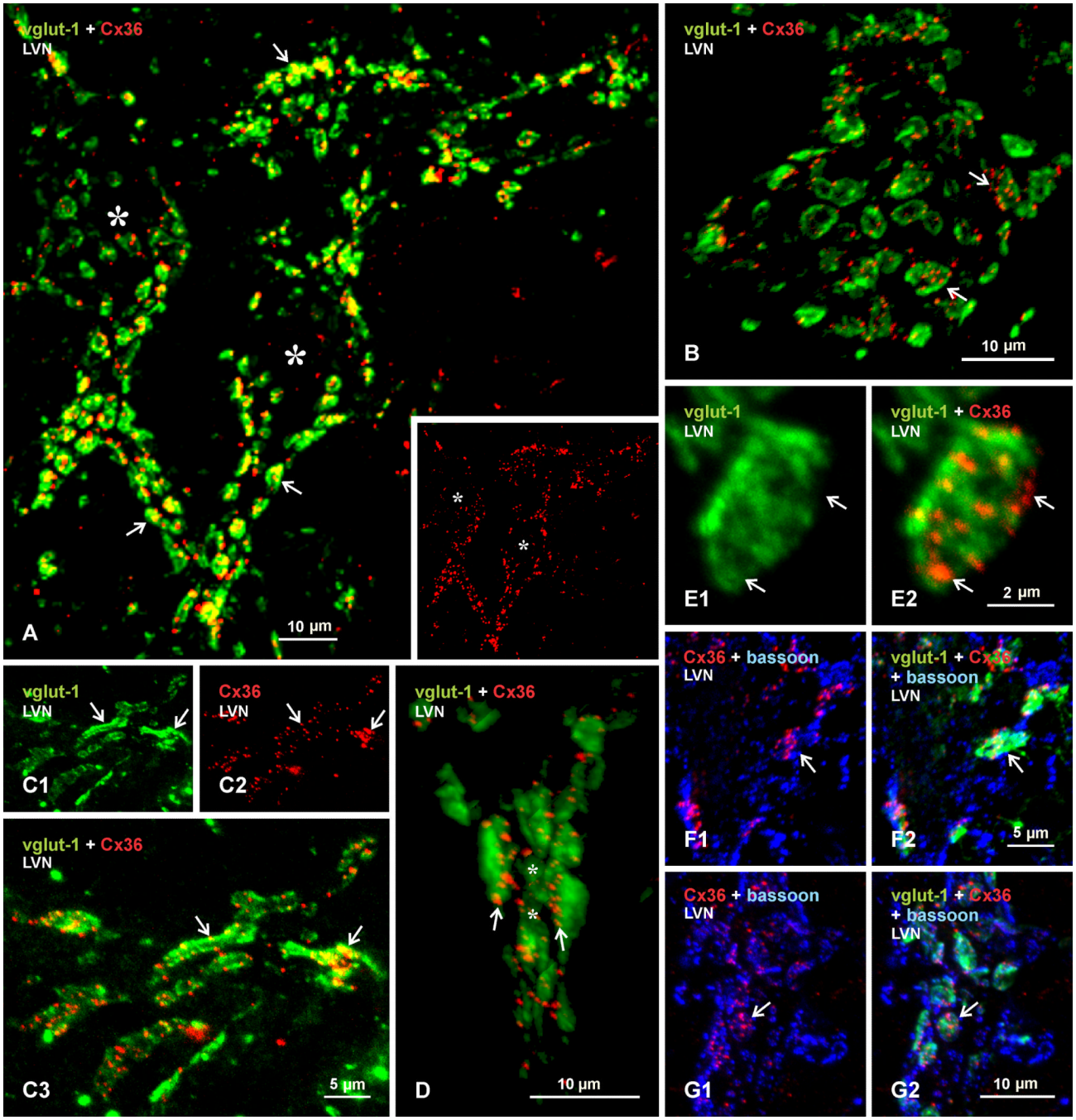

Fig. 7.

Laser scanning confocal double immunofluorescence labelling of Cx36 with vglut-1 or bassoon in the LVN of adult rat. (A) Low magnification showing two neuronal somata (asterisks) and their large initial dendrites densely covered by large vglut-1-positive (green) nerve terminals (arrows), with labelling for Cx36 (red, shown alone in the same field in inset) associated with most of these terminals (yellow in overlay). (B) Higher magnification of another LVN neuronal somata, showing clusters of Cx36-puncta associated with many of the vglut-1-positive terminals (arrows). (C) Section through occasionally seen extended segments of vglut-1-positive terminal contacts (C1, arrows), with Cx36-puncta distributed along the length of these segments (C2, arrows), as seen by yellow in overlay (C3, arrows).

(D) Labelling for Cx36 and vglut-1 in a 3D-rendered image from a Z-stack scan of 6 μ through an initial dendrite segment surrounded by vglut-1-positive terminals, showing localization of Cx36-puncta at the surface of vglut-1-positive terminal contacts with the dendritic shaft (arrows). (E) Magnification of a single vglut-1-positive terminal (E1) and, in the same field, its associated cluster of Cx36-puncta (E2), showing localization of puncta in regions of lower vglut-1 labelling density (arrows). (F,G) Triple immunofluorescence labelling for Cx36 (red), vglut-1 (green) and the active zone marker bassoon (blue), showing two examples of Cx36-puncta intermingled with punctate labelling for bassoon in red/blue overlay (F1 and G1, arrows), and co-localization of Cx36/bassoon with labelling for vglut-1 in red/blue/green overlay (F2 and G2, arrows).

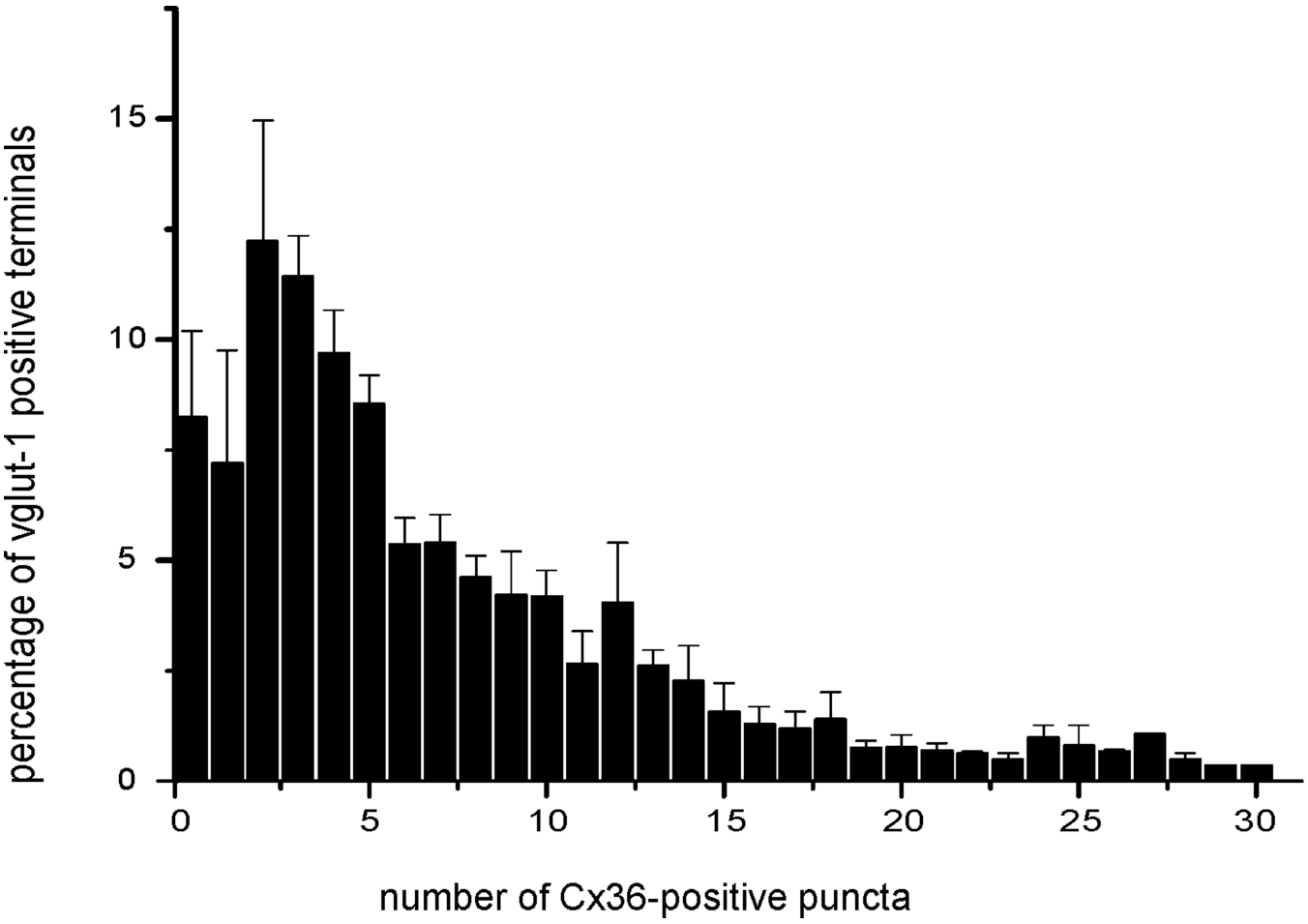

Fig. 8.

Histogram showing range in numbers of Cx36-puncta associated with large vglut-1-positive terminals on neurons in the LVN of adult rat. The greatest percentage of terminals have between three to five Cx36-puncta. Data were plotted from counts of a total of 5,836 Cx36-puncta localized to a total of 932 terminals in four rats, and expressed as percentage of terminals (mean ± s.e.m.) displaying the number of puncta indicated.

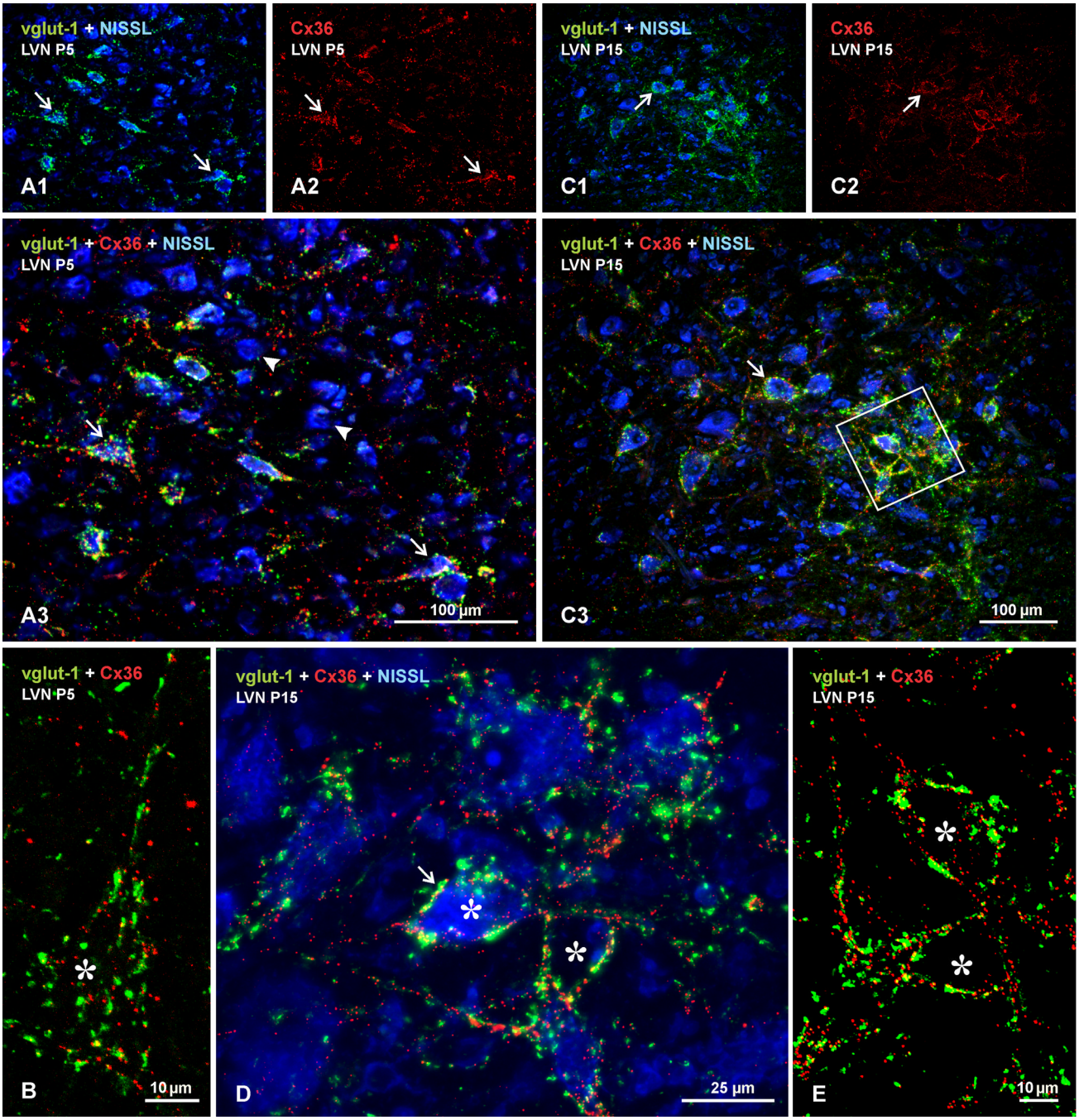

Fig. 9.

Developmental appearance of immunolabelling for Cx36 and vglut-1 in LVN of rat at postnatal day 5 and 15. Sections were labelled for Cx36 (red) and vglut-1 (green), with Nissl fluorescence counterstain (blue). (A,B) Postnatal day 5 LVN, shown at low magnification (A) and a confocal image of a single neuron (marked by asterisk) at higher magnification (B). A sparse to moderate density of vglut-1-positive terminals is seen on LVN neuronal somata (A1, arrows) and less so on dendrites, and a similar distribution of labelling for Cx36 is seen on these somata, as shown by labelling for Cx36 alone (A2, arrows), with moderate degree of co-localization, as seen in red/green/blue overlay (A3, arrows). Many neurons are nearly devoid of Cx36/vglut-1 labelling (arrowheads), and some dispersed Cx36-puncta

appear unassociated with vglut-1 (B) or with Nissl-stained neurons (A3). (C–E) Postnatal day 15 LVN at low magnification (C), with boxed area in C3 shown as higher magnification confocal image in D, and the boxed area in D shown with only red/green overlay in E. Labelling for vglut-1 (C1) and Cx36 (C2) is increased compared to postnatal day 5, but is still only moderate on neuronal somata and dendritic initial segments (C3, arrows). Labelling for Cx36 appears on cell bodies and dendrites often as individual puncta rather than as clusters, dispersed Cx36-puncta not associated with Nissl-stained neurons is reduced (D,E), and degree of Cx36/vglut-1 co-localization (arrow) is modest compared with that seen in adult.

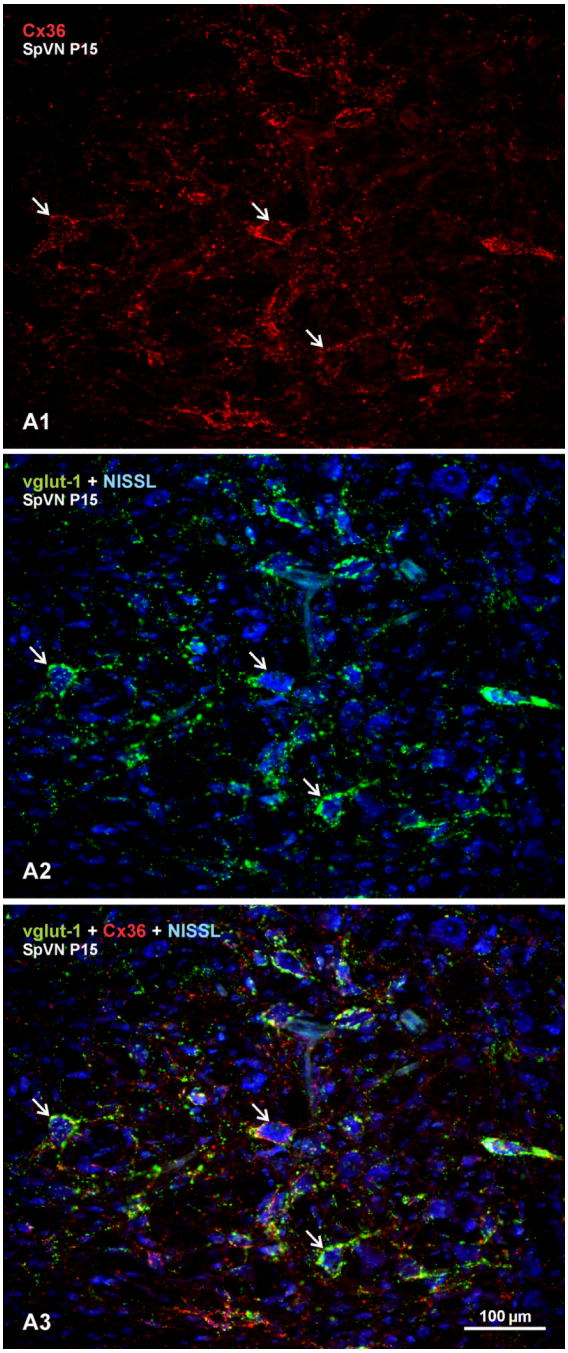

Fig. 10.

Developmental appearance of immunolabelling for Cx36 and vglut-1 in SpVN of rat at postnatal day 15. (A) Images of the same field labelled for Cx36 (red) and vglut-1 (green), with Nissl fluorescence counterstain (blue). Labelling for Cx36 (A1, arrows) and vglut-1 (A2, arrows) is dense on neuronal somata and moderate on initial dendritic segments. Cx36-puncta appear as clusters of puncta co-localized with vglut-1 on neuronal somata (A3, arrows) or as non-colocalized puncta, and dispersed Cx36-puncta not associated with Nissl-stained neurons are readily evident.

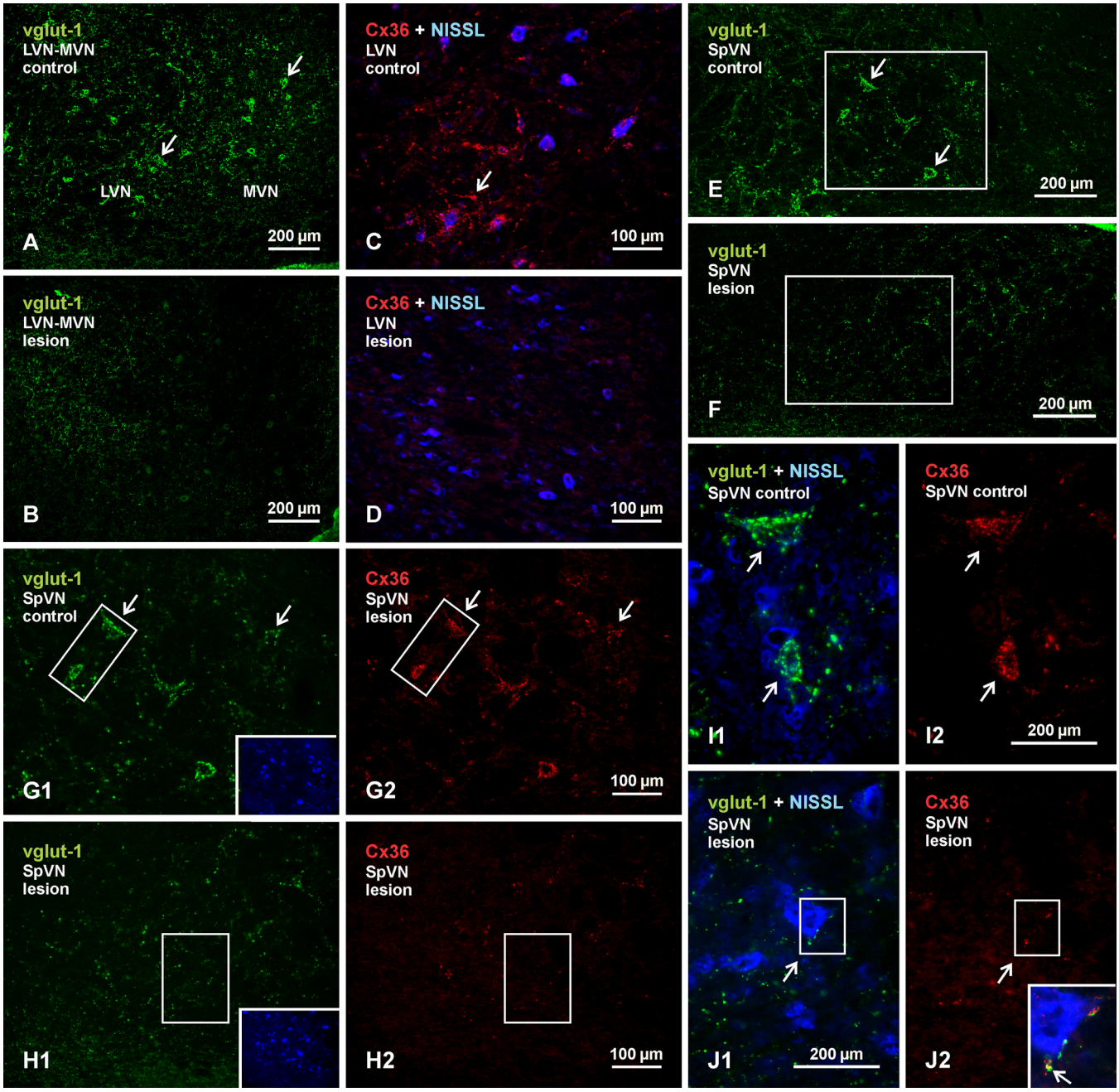

Fig. 11.

Immunofluorescence labelling of vglut-1 and Cx36 in the vestibular nuclei of adult rat after unilateral vestibular nerve section and Scarpa ganglionectomy. Pairs of images display control (left side) *vs.* deafferented (right side) vestibular nuclei, and each pair was acquired from areas ipsilateral and contralateral to the side of the lesion from the same animal. (A,B) Images of the LVN and the lateral portion of MVN, showing dense labelling of vglut-1 around neuronal somata on the control side (A, arrows) and a loss of this labelling around somata on the lesioned side. (C,D) Higher magnification of the LVN with blue Nissl counterstaining, showing dense collections of Cx36-puncta on the control side (C, arrow) and depletion of these puncta on the lesioned side (D). (E,F) Images showing labelling of vglut-1 associated with neurons in the SpVN on the control side (E, arrows) and a loss of

this labelling on the lesion side (F). (G,H) Images of labelling for vglut-1 (G1) and Cx36 (G2) in the same field of SpVN taken from the boxed area in E, and of vglut-1 (H1) and Cx36 (H2) in the same field taken from the boxed area in F. Insets show the two fields with blue Nissl counterstaining of neurons. Vglut-1 and Cx36 associated with neuronal somata on the control side (G1,G2, arrows) is depleted on the lesion side H1,H2). (I,J) Magnifications of the boxed areas from G1 and G2 are shown in I1 and I2, respectively, and those from H1 and H2 are shown in J1 and J2, respectively. Labelling of large vglut-1-positive terminals associated with neuronal somata (blue Nissl counterstained) on the control side (I1, arrows) are absent or reduced in size on the lesion side (J1, arrow), and Cx36-puncta associated with these terminals (I2, arrows) are similarly depleted or reduced in number (J2, arrow). The few shrunken terminals left on the lesion side remain co-localized with Cx36, as shown by overlay of the boxed areas in J1 and J2 (shown in inset in J2, with red/green overlay seen a yellow, arrow).